



# Transition Energies and Line Oscillator Strengths of the $C^2\Pi(0)$ - $X^2\Pi(0-6)$ Absorption Bands of Nitric Oxide. A Theoretical Study

C. Lavín and A. M. Velasco

Departamento de Química Física y Química Inorgánica, Facultad de Ciencias, Universidad de Valladolid, E-47005 Valladolid, Spain; [clavin@qf.uva.es](mailto:clavin@qf.uva.es)

Received 2022 July 25; revised 2022 October 25; accepted 2022 October 26; published 2022 December 9

## Abstract

Theoretical absorption oscillator strengths and wavelengths for rotational transitions of the  $C^2\Pi(v' = 0)$ - $X^2\Pi(v'')$  bands with  $v'' = 0-6$  of nitric oxide are reported. The Molecular Quantum Defect Orbital method has been used in the calculations and the known interaction between the  $C^2\Pi(v = 0)$  Rydberg and the  $B^2\Pi(v = 7)$  valence states has been dealt with through an appropriate rovibronic energy matrix. We hope that the reported data may be useful in the analysis of the observed ultraviolet nightglow emission from nitric oxide in the upper atmospheres of Earth, Venus, and Mars.

*Unified Astronomy Thesaurus concepts:* Molecular spectroscopy (2095); Line intensities (2084); Line positions (2085)

## 1. Introduction

The nitric oxide radical (NO), although it is a minor constituent, plays an important role in the Earth's atmosphere due to the numerous chemical and physical processes in which it is involved. NO has also been detected in the upper atmospheres of Venus and Mars. In addition, NO is a fairly abundant molecule in the interstellar medium (ISM) where it is considered an important precursor in the formation of more complex nitrogen-bearing species (Joshi et al. 2012). It was first identified in the ISM toward Sgr B2 by Liszt & Turner (1978). Since then, it has been detected in several molecular clouds (McGonagle et al. 1990; Ziurys et al. 1991; Gerin et al. 1992), in a circumstellar envelope (Quintana-Lacaci et al. 2013), and in an extragalactic source (Martin et al. 2003).

The  $C^2\Pi$ - $X^2\Pi$  band system of NO, also named the  $\delta$ -band system, is of interest in the analysis of molecular emission observations in the ultraviolet (UV) spectra of planetary atmospheres where nitric oxide is present. In particular, several bands belonging to the  $C^2\Pi(v' = 0)$ - $X^2\Pi(v'')$  progression, which are the object of the present study, have been observed in the UV spectra from atmospheres of Earth, Venus, and Mars. The  $C^2\Pi(0)$ - $X^2\Pi(0-3)$  bands were identified in the ultraviolet spectra from the atmospheric nightglow of Earth obtained by balloon-borne (Cohen-Sabban & Vuillemin 1973) and rocket-borne (Feldman & Takacs 1974) spectrometers. Afterward, Eastes et al. (1992) analyzed the Earth's nightglow spectra observed from the S3-4 satellite and detected the  $v'' = 0-6$  bands of the  $C^2\Pi(0)$  progression. First observations of the  $\delta$  bands of NO in the ultraviolet (UV) nightglow of Venus were performed by Feldman et al. (1979) using the International Ultraviolet Explorer (IUE) and by Stewart & Barth (1979) with the Pioneer Venus Orbiter. Feldman et al. (1979) identified the features observed at 1909, 1980, and 2055 Å in Venus's UV emission spectra as the  $C^2\Pi(0)$ - $X^2\Pi(0)$ ,  $C^2\Pi(0)$ - $X^2\Pi(1)$ , and  $C^2\Pi(0)$ - $X^2\Pi(2)$  bands of NO, respectively. From their analysis of the nightglow of Venus, Stewart & Barth (1979) concluded that the

spectrum contains six clearly identifiable bands, which belong to the  $C^2\Pi(0)$ - $X^2\Pi(v'')$  progression with  $v'' = 0-5$ . Later, Gérard et al. (2008) detected the  $C^2\Pi(0)$ - $X^2\Pi(0-8)$  bands in the Venusian nightglow spectra obtained with the Spectroscopy for Investigation of Characteristic of the Atmosphere of Venus (SPICAV) spectrometer on board Venus Express spacecraft. More recently, Bertaux (2005) identified the  $C^2\Pi(0)$ - $X^2\Pi(0-6)$  bands of nitric oxide in the Martian nightglow spectra obtained with SPICAM (Spectroscopy for the Investigation of the Characteristics of the Atmosphere of Mars) UV spectrometer on board Mars Express. The quantitative interpretation of the atmospheric observations and, further, the modeling of atmospheric processes require an accurate knowledge of the UV spectrum of NO molecule. It is essential to measure its atmospheric abundance precisely to understand the atmospheric chemistry; this requires reliable NO molecule line parameters, including line positions and intensities (Dana et al. 1994).

Several spectroscopic studies have been performed on the  $C^2\Pi(0)$ - $X^2\Pi(v'')$  progression of NO since Herzberg et al. (1956) analyzed the rotational structure of the absorption  $C^2\Pi(0)$ - $X^2\Pi(0)$  band and determined the rotational constant of the  $C^2\Pi(0)$  state. Lagerqvist & Miecher (1958) reported the rotational line positions of this band and pointed out the mutual perturbation between the  $C^2\Pi(0)$  Rydberg and  $B^2\Pi(7)$  valence states. Ackerman & Miescher (1969) photographed with high resolution the emission  $C^2\Pi(0)$ - $X^2\Pi(0)$  and  $C^2\Pi(0)$ - $X^2\Pi(1)$  bands and assigned the rotational lines to the observed branches. Scheingraber & Vidal (1985) found the  $C^2\Pi(0)$  progression from  $v'' = 0$  to  $v'' = 8$  in their one-photon laser-induced fluorescence excitation studies of the  $A^2\Sigma^+$ ,  $B^2\Pi$ ,  $C^2\Pi$ , and  $D^2\Sigma^+$  states of NO. Murray et al. (1994) measured accurate line positions of the  $C^2\Pi(0)$ - $X^2\Pi(0)$  band with a vacuum ultraviolet (VUV) Fourier transform (FT) spectrometer. They also determined rovibronic term values up to  $J = 19.5$  for the  $C^2\Pi(v = 0)$  state. Later, Braun et al. (2000) derived term values up to  $J = 26.5$  for the  $v = 0$  level of the  $C^2\Pi$  state, from observed transitions in emission with Fourier transform spectrometry. Rotational levels of the  $X^2\Pi$  ground state, up to  $v = 22$ , were obtained from the vibration-rotation emission spectrum of NO registered by Amiot (1982) using a high-resolution Fourier transform interferometer. Hinz et al. (1986) reported



Original content from this work may be used under the terms of the [Creative Commons Attribution 4.0 licence](#). Any further distribution of this work must maintain attribution to the author(s) and the title of the work, journal citation and DOI.

rotation energies for the  $v = 0$  and  $v = 1$  levels of the ground state obtained from heterodyne frequency measurements on the fundamental band of nitric oxide. Very recently, Qu et al. (2021a) published high-accuracy line positions for the  $C^2\Pi(0)-X^2\Pi(v'')$  progression of NO as part of the ExoMol project.

Regarding absorption oscillator strengths, or  $f$ -values, the experimental research so far performed has been focused on the  $C^2\Pi(0)-X^2\Pi(0)$  band. A summary of the experimental oscillator strength data of that band reported in the literature before 2006 can be found in the paper of Yoshino et al. (2006). The most recent experimental band  $f$ -values were obtained by Yoshino et al. (2006) with a combination of vacuum ultraviolet Fourier transform spectrometry and synchrotron radiation, and by Kato et al. (2007) using electron energy loss spectroscopy. On the theoretical part, Galluser & Dressler (1982) calculated the  $f$ -value for the  $C^2\Pi(0)-X^2\Pi(0)$  band in a basis of electronically coupled diabatic states. De Vivie & Peyerimhoff (1988) determined  $f$ -values for the  $C^2\Pi(0)-X^2\Pi(0-6)$  bands using a multireference configuration interaction method. Subsequently, Velasco et al. (2010) calculated  $f$ -values for the  $C^2\Pi(0)-X^2\Pi(0-10)$  bands with the Molecular Quantum Defect Orbital (MQDO) approach. Very recently, Zammit et al. (2022) calculated the rotationally averaged absorption oscillator strength for the  $C^2\Pi(0)-X^2\Pi(0)$  transition using the complete active space self-consistent field (CAS-MRCI) technique. All of the measurements and calculations so far mentioned, supplied transition oscillator strengths with vibrational but not rotational resolution. The first high-resolution absorption integrated cross sections of the  $C^2\Pi(0)-X^2\Pi(0)$  rotational lines were reported by Murray et al. (1994) by using a VUV FT spectrometer. In a later work, Yoshino et al. (2006) obtained ultrahigh-resolution cross-section measurements by using the combination of a VUV FT spectrometer and a synchrotron radiation source. Mayor et al. (2005) calculated rotational line-integrated photoabsorption cross sections for the rotational lines of the  $C^2\Pi(0)-X^2\Pi(0)$  band with the Molecular Quantum Defect Orbital (MQDO) approach. Chauveau et al. (2002) have calculated the absorption coefficient for spectral lines of the  $\delta$  band system at different temperatures. Qu et al. (2021a) reported Einstein emission coefficients for the rovibronic  $C^2\Pi-X^2\Pi$  system obtained through a mixture of empirical and theoretical electronic transition dipole moments.

As reported above, most of the work of both experimentalists and theoreticians regarding the rotational structure of the  $C^2\Pi(0)-X^2\Pi(v'')$  progression has focused on the  $C^2\Pi(0)-X^2\Pi(0)$  or  $\delta(0,0)$  band. Thus, in order to achieve a better understanding of UV molecular emission observations in the Earth, Venus, and Mars atmospheres, where several bands of the  $C^2\Pi(0)$  progression of NO have been detected, in this work we have calculated line  $f$ -values and wavelengths for the twelve branches of the  $C^2\Pi(0)-X^2\Pi(0-6)$  bands. It is well known that the  $v = 0$  level of the Rydberg  $C^2\Pi$  state is homogeneously perturbed by the  $v = 7$  level of the valence  $B^2\Pi$  state (Lagerqvist & Miecher 1958; Galluser & Dressler 1982). In our calculations, we have taken into account this perturbation through an appropriate rovibronic energy matrix. The Rydberg  $C^2\Pi$  state has been described with the Molecular Quantum Defect Orbital (MQDO) method, which has proved to yield good quality rovibronic oscillator strengths of diatomic

molecules in previous works (Lavín & Velasco 2011; Velasco & Lavín 2020).

## 2. Method of Calculation

For a transition to a given rovibronic level  $v'J'$  in the final electronic state from a rovibronic level  $v''J''$  in the initial electronic state, in a diatomic molecule, the absorption oscillator strength is defined through the following expression (Larsson 1983):

$$f_{v'J',v''J''} = \frac{8\pi^2 m c a_0^2}{3h} \nu_{v'J',v''J''} \frac{S_{J'J''}}{2J'' + 1}, \quad (1)$$

where  $f_{v'J',v''J''}$  is dimensionless,  $\nu_{v'J',v''J''}$  is the frequency of the rotational line in  $\text{cm}^{-1}$  and  $S_{J'J''}$  is the rotational line strength in atomic units.

Assuming the validity of the Born–Oppenheimer approximation and the fact that the nuclear term of the wave function can be approximated by the product of rotational and vibrational wave functions, the rotational line strength can be expressed in this way (Whiting & Nicholls 1974):

$$S_{J'J''} = q_{v'v''} R_e^2 \mathcal{J}_{J'J''}, \quad (2)$$

where  $q_{v'v''}$  is the Franck–Condon factor (FFC), which is given by the square of the vibrational overlap integral,  $R_e$  is the electronic transition moment (in atomic units) and  $\mathcal{J}_{J'J''}$  is the Hönl–London factor, which accounts for the relative rotational line strength within the vibronic manifold of each one of the rovibronic transitions. In this work, the equations reported by Kovács (1969) are used to obtain the Hönl–London factors for each branch of the studied bands.

The FFC is calculated from vibrational wave functions of the two electronic states involved in the transition, using the Rydberg–Klein–Rees (RKR; Rydberg 1931, Klein 1932, Rees 1947) approach. We use the Numerov algorithm to solve the Schrödinger equation over the potential energy curve of the electronic states of the transition.

The electronic transition moment,  $R_e$ , is calculated by using the MQDO method, which was developed within our group (Martín et al. 1996) to study molecular Rydberg transitions. In this method, the MQDO wave functions are expressed as

$$\psi(r, \vartheta, \varphi)_{nl\mu\nu} = \frac{1}{r} R(r)_{nl\mu} \Xi(\vartheta, \varphi)_{l\mu\nu}, \quad (3)$$

where  $n$  and  $l$  are the principal and orbital angular momentum quantum numbers, respectively,  $\mu$  labels the irreducible representation of the molecular symmetry group and  $\nu$  identifies the basis function of this representation.  $\Xi(\vartheta, \varphi)_{l\mu\nu}$  is the angular part of the MQDO wave functions, and it is expressed as a linear combination of spherical harmonics adapted to the molecular symmetry. The radial part of the MQDO wave functions,  $R(r)_{nl\mu}$ , is the analytical solution of a one-electron Schrödinger equation that contains an effective central field potential. This parametric potential accounts for electron correlation and is defined as:

$$V(r) = \frac{(c - \delta)(2l + c - \delta + 1)}{2r^2} - \frac{1}{r}, \quad (4)$$

where  $\delta$  is the quantum defect and  $c$  is an integer within a narrow range of values that ensures the normalizability of the

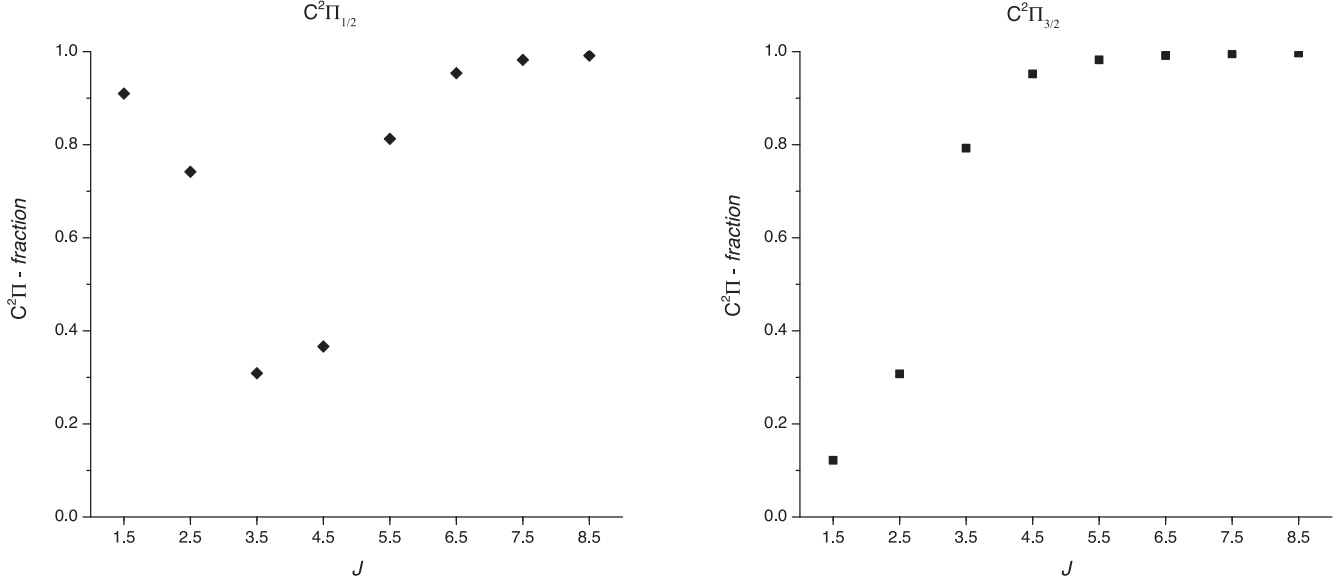


**Figure 1.**  $C^2\Pi$ -fraction of the  $C^2\Pi_{1/2}$  and  $C^2\Pi_{3/2}$  rotational levels of NO calculated from the state mixing model, as discussed in the text.

molecular orbitals and their right nodal pattern. In this way, we can formulate separately the radial and angular contributions to the transition moment so that for a transition between two unperturbed electronic states  $i$  and  $j$ , it is expressed as follows:

$$R_e^2 = Q\{i \rightarrow j\} R_{ij}(r)^2, \quad (5)$$

where  $Q\{i \rightarrow j\}$  is the angular factor resulting from the integration of the angular functions and the transition operator and  $R_{ij}(r)$  is the radial transition moment. An important computational advantage of the MQDO approach is that the transition integral results in closed-form analytical expression.

### 3. Results and Discussion

At the equilibrium geometry, the ground state electronic configuration of the NO molecule is  $(1\sigma)^2(2\sigma)^2(3\sigma)^2(4\sigma)^2(1\pi)^4(5\sigma)^2(2\pi)^1X^2\Pi$ . The  $C^2\Pi$  state is the first member of the  $np\pi$  Rydberg series of NO and corresponds to the excitation of the unpaired electron in the  $2\pi$  orbital to a  $3p\pi$  orbital. The rotational levels of the Rydberg  $C^2\Pi$  state are characterized by both spin-splitting and  $\Lambda$ -doubling.

Early rotational analysis of the absorption spectrum of NO carried out by Lagerqvist & Miecher (1958) showed that the  $C^2\Pi(0)$  Rydberg state is perturbed by the  $B^2\Pi(7)$  valence state. Since then, there have been several studies on the homogeneous Rydberg–valence interaction in NO. A study, including homogeneous and heterogeneous perturbations between the  $B^2\Pi(v=7, 8, 9, 10)$  vibrational levels and the  $v=0$  levels of the  $C^2\Pi(3p\pi)$  and  $D^2\Sigma^+(3p\sigma)$  Rydberg states, was performed by Amiot & Verges (1982). Their perturbation analysis showed that, for low-lying  $J$ , the  $C^2\Pi(0)$  state is perturbed by the  $B^2\Pi(7)$  state, while for values of  $J$  around 30 it is perturbed by the  $B^2\Pi(v=8, 9)$  levels. In this work, we studied rovibronic transitions to the  $C^2\Pi_{1/2}(0)$  and  $C^2\Pi_{3/2}(0)$  substates up to  $J=20.5$ ; therefore, in our calculations we considered only the homogeneous interaction between the two doublet components of the  $C^2\Pi(0)$  state and the two doublet components of the  $B^2\Pi(7)$  state.

In this work, we have used the method of matrix diagonalization to describe the Rydberg–valence interaction.

In this method, one starts with an appropriate basis set of diabatic states and construct the matrix of the molecular Hamiltonian, whose diagonal elements are the unperturbed rotational energies of the states involved in the interaction and whose off-diagonal elements are the coupling parameters, which may be written as

$$H^{ee'}_{vv'} = H^{ee'} S^{ee'}_{vv'}, \quad (6)$$

where  $H^{ee'}$ , the interaction energy of the  $e'$  and  $e''$  electronic states, is an adjustable parameter, and  $S^{ee'}_{vv'}$  is the vibrational overlap integral (Carroll & Hagim 1988). The diagonalization of the interaction matrix yields the eigenvalues and eigenvectors of the perturbed states. So, the Rydberg–valence interaction of the  $C^2\Pi(0)$  and  $B^2\Pi(7)$  levels is presently treated through a  $4 \times 4$  interaction matrix for each  $\Lambda$  doubling component and value of  $J$ . The diagonal elements are the unperturbed rotational energies of the four  $C^2\Pi_{1/2}(0)$ ,  $C^2\Pi_{3/2}(0)$ ,  $B^2\Pi_{1/2}(7)$ ,  $B^2\Pi_{3/2}(7)$  states involved in the interaction. The off-diagonal matrix elements are the coupling parameters of the  $B^2\Pi(7)$  and  $C^2\Pi(0)$  states. The calculation of the energies of the unperturbed states requires accurate values of the following spectroscopic parameters: the vibronic energy  $T_v$ , the spin–orbit constant  $A$ , the rotational distortion constant  $D$ , and the  $\Lambda$ -doubling parameters  $p$  and  $q$  for the  $C^2\Pi(0)$  and  $B^2\Pi(7)$  levels. Very accurate values for the molecular constants of the  $C^2\Pi(0)$  level were obtained by Amiot & Verges (1982), who carried out a deperturbation procedure of the  $B^2\Pi$  and  $C^2\Pi$  levels through the emission spectrum of the  $C^2\Pi(0)$ - $A^2\Sigma^+(0)$  and  $D^2\Sigma^+(0)$ - $A^2\Sigma^+(0)$  transitions measured at very high resolution using Fourier transform spectrometry. Murray et al. (1994) measured in absorption the fine structure of the  $B^2\Pi(7)$ - $X^2\Pi(0)$  and  $C^2\Pi(0)$ - $X^2\Pi(0)$  transitions by using a vacuum ultraviolet Fourier transform spectrometer. These authors carried out a simultaneous analysis of both transitions for which they adopted the deperturbation procedure developed by Amiot & Verges (1982). Murray et al. (1994) claim that their results for the  $B^2\Pi(7)$  state are more accurate than the

**Table 1**  
Transition Energies (in Å) and Line Oscillator Strengths for  $P_{11}$ ,  $P_{12}$ ,  $P_{22}$ , and  $P_{21}$  branches of the  $C^2\Pi(0)-X^2\Pi(0)$  band of NO.

		$P_{11}$			$P_{12}$			$P_{22}$			$P_{21}$		
		$\lambda^a$	$f^a$	$f^b$									
4	2.5	1909.61	9.6E-04	6.7E-04 1.3E-03	1914.00	6.8E-04	4.5E-04	1913.56	1.3E-04	7.0E-04 3.8E-05	1909.17	2.0E-04	1.4E-05
	3.5	1909.64	9.5E-04	8.1E-04 1.2E-03	1914.04	7.3E-04	5.8E-04	1913.76	3.9E-04	6.5E-04 2.3E-04	1909.36	4.3E-04	4.2E-04 1.3E-04
	4.5	1909.77	5.0E-04	8.6E-04 7.1E-04	1914.19	3.8E-04	1.7E-04 1.6E-04	1913.88	1.0E-03	1.0E-03 8.1E-04	1909.47	9.3E-04	7.0E-04 6.3E-04
	5.5	1910.01	6.1E-04	1.1E-03 7.6E-04	1914.45	4.4E-04	2.7E-04 1.4E-05	1913.89	1.2E-03	1.2E-03 1.1E-03	1909.45	1.0E-03	8.0E-04 8.8E-04
	6.5	1910.20	1.2E-03	1.2E-03 1.3E-03	1914.66	8.5E-04	5.0E-04 4.9E-04	1913.84	1.4E-03	1.3E-03 1.3E-03	1909.39	1.0E-03	9.3E-04 9.3E-04
	7.5	1910.28	1.4E-03	1.3E-03 1.4E-03	1914.77	9.4E-04	6.1E-04 7.6E-04	1913.78	1.4E-03	1.3E-03 1.4E-03	1909.29	1.0E-03	9.7E-04 9.4E-04
	8.5	1910.31	1.5E-03	1.3E-03 1.5E-03	1914.83	9.4E-04	7.3E-04 8.3E-04	1913.69	1.5E-03	1.5E-03 1.4E-03	1909.17	9.8E-04	1.0E-03 9.2E-04
	9.5	1910.32	1.6E-03	1.5E-03 1.5E-03	1914.87	9.2E-04	8.8E-04 8.4E-04	1913.58	1.5E-03	1.8E-03 1.5E-03	1909.03	9.5E-04	1.1E-03 9.0E-04
	10.5	1910.30	1.6E-03	1.5E-03 1.6E-03	1914.89	8.9E-04	9.3E-04 8.4E-04	1913.44	1.6E-03	1.9E-03 1.6E-03	1908.87	9.1E-04	9.7E-04 8.8E-04
	11.5	1910.26	1.7E-03	1.6E-03 1.6E-03	1914.88	8.6E-04	1.0E-03 8.2E-04	1913.29	1.6E-03	2.0E-03 1.6E-03	1908.68	8.8E-04	9.3E-04 8.6E-04
	12.5	1910.19	1.7E-03	1.5E-03 1.7E-03	1914.86	8.4E-04	9.4E-04 8.0E-04	1913.12	1.7E-03	2.1E-03 1.6E-03	1908.47	8.5E-04	9.6E-04 8.3E-04
	13.5	1910.10	1.7E-03	1.5E-03 1.7E-03	1914.81	8.1E-04	8.1E-04 7.8E-04	1912.93	1.7E-03	2.2E-03 1.7E-03	1908.23	8.3E-04	1.0E-03 8.0E-04
	14.5	1909.99	1.8E-03	1.5E-03 1.7E-03	1914.74	7.8E-04	7.8E-04 7.6E-04	1912.72	1.7E-03	2.3E-03 1.7E-03	1907.97	8.0E-04	1.1E-03 7.8E-04
	15.5	1909.85	1.8E-03	1.7E-03 1.8E-03	1914.66	7.6E-04	7.5E-04 7.4E-04	1912.49	1.8E-03	2.3E-03 1.8E-03	1907.69	7.7E-04	1.3E-03 7.5E-04
	16.5	1909.69	1.8E-03	1.8E-03 1.8E-03	1914.55	7.3E-04	7.0E-04 7.1E-04	1912.23	1.8E-03	2.3E-03 1.8E-03	1907.39	7.4E-04	1.3E-03 7.3E-04
	17.5	1909.51	1.9E-03	1.8E-03 1.8E-03	1914.42	7.1E-04	6.9E-04	1911.96	1.8E-03	2.1E-03 1.8E-03	1907.07	7.2E-04	1.4E-03 7.0E-04
	18.5	1909.31	1.9E-03	1.8E-03 1.9E-03	1914.28	6.8E-04	6.7E-04	1911.67	1.9E-03	1.9E-03	1906.72	6.9E-04	1.4E-03 6.8E-04
	19.5	1909.08	1.9E-03	1.9E-03	1914.11	6.6E-04	6.5E-04	1911.36	1.9E-03	1.9E-03	1906.35	6.7E-04	6.6E-04
	20.5	1908.84	1.9E-03	1.9E-03	1913.92	6.4E-04	6.3E-04	1911.03	1.9E-03	1.9E-03	1905.96	6.4E-04	6.3E-04

**Notes.**<sup>a</sup> This work.<sup>b</sup> First entry: deduced from integrated cross sections of Yoshino et al. (2006). Second entry: deduced from Einstein emission coefficients of Qu et al. (2021a).

**Table 2**  
Transition Energies (in Å) and Line Oscillator Strengths for  $R_{11}$ ,  $R_{12}$ ,  $R_{22}$ , and  $R_{21}$  branches of the  $C^2\Pi(0)-X^2\Pi(0)$  band of NO

$J''$	$R_{11}$				$R_{12}$				$R_{22}$				$R_{21}$			
	$\lambda^a$	$f^a$	$f^b$	$\lambda^a$	$f^a$	$f^b$	$\lambda^a$	$f^a$	$f^b$	$\lambda^a$	$f^a$	$f^b$	$\lambda^a$	$f^a$	$f^b$	
1.5	1908.91	1.3E-03	1.9E-03 1.7E-03	1913.29	8.7E-04	6.0E-04	1913.00	4.1E-04	2.4E-04	1908.63	6.4E-04	3.3E-04 2.0E-04				
2.5	1908.79	6.1E-04	1.6E-03 9.4E-04	1913.18	4.8E-04	1.7E-04	1912.88	1.1E-03	9.2E-04 9.2E-04	1908.49	1.3E-03	8.6E-04 8.7E-04				
3.5	1908.79	7.1E-04	1.4E-03 9.3E-04	1913.19	5.5E-04	2.4E-05	1912.63	1.4E-03	1.3E-03 1.3E-03	1908.23	1.4E-03	1.1E-03 1.1E-03				
4.5	1908.73	1.4E-03	1.4E-03 1.5E-03	1913.15	1.1E-03	5.5E-04 6.2E-04	1912.33	1.5E-03	1.4E-03 1.4E-03	1907.92	1.3E-03	1.1E-03 1.2E-03				
5.5	1908.57	1.6E-03	1.4E-03 1.6E-03	1913.00	1.1E-03	9.2E-04 9.3E-04	1912.02	1.6E-03	1.4E-03 1.5E-03	1907.59	1.2E-03	1.1E-03 1.2E-03				
6.5	1908.36	1.6E-03	1.5E-03 1.6E-03	1912.82	1.1E-03	1.0E-03 1.0E-03	1911.67	1.6E-03	1.5E-03 1.6E-03	1907.22	1.2E-03	1.0E-03 1.1E-03				
7.5	1908.12	1.7E-03	1.7E-03 1.7E-03	1912.60	1.1E-03	1.1E-03 1.0E-03	1911.31	1.6E-03	1.5E-03 1.6E-03	1906.84	1.1E-03	9.8E-04 1.1E-03				
8.5	1907.86	1.7E-03	1.5E-03 1.7E-03	1912.37	1.1E-03	1.1E-03 9.9E-04	1910.93	1.7E-03	1.6E-03 1.7E-03	1906.43	1.1E-03	1.0E-03 1.0E-03				
9.5	1907.58	1.7E-03	1.5E-03 1.7E-03	1912.11	1.0E-03	8.9E-04 9.7E-04	1910.53	1.7E-03	1.5E-03 1.7E-03	1906.00	1.0E-03	9.9E-04 1.0E-03				
10.5	1907.27	1.8E-03	1.5E-03 1.8E-03	1911.84	9.8E-04	9.0E-04 9.4E-04	1910.11	1.7E-03	1.6E-03 1.7E-03	1905.54	1.0E-03	9.5E-04 9.8E-04				
11.5	1906.93	1.8E-03	1.6E-03 1.8E-03	1911.54	9.4E-04	7.3E-04 9.1E-04	1909.67	1.8E-03	1.5E-03 1.8E-03	1905.07	9.6E-04	8.1E-04 9.4E-04				
12.5	1906.58	1.8E-03	1.6E-03 1.8E-03	1911.23	9.0E-04	7.2E-04 8.8E-04	1909.21	1.8E-03	1.7E-03 1.8E-03	1904.57	9.2E-04	7.8E-04 9.1E-04				
13.5	1906.20	1.9E-03	1.7E-03 1.9E-03	1910.89	8.7E-04	7.4E-04 8.6E-04	1908.73	1.8E-03	1.8E-03 1.8E-03	1904.05	8.9E-04	7.3E-04 8.7E-04				
14.5	1905.80	1.9E-03	1.7E-03 1.9E-03	1910.54	8.4E-04	7.0E-04 8.3E-04	1908.23	1.9E-03	2.0E-03 1.9E-03	1903.50	8.5E-04	7.7E-04 8.4E-04				
15.5	1905.38	1.9E-03	2.1E-03 1.9E-03	1910.16	8.1E-04	7.7E-04 8.0E-04	1907.71	1.9E-03	2.0E-03 1.9E-03	1902.94	8.2E-04	7.7E-04 8.1E-04				
16.5	1904.93	1.9E-03	1.9E-03 1.9E-03	1909.77	7.8E-04	7.3E-04 7.7E-04	1907.17	1.9E-03	1.9E-03 1.9E-03	1902.35	7.9E-04	6.7E-04 7.8E-04				
17.5	1904.47	2.0E-03	2.0E-03 2.0E-03	1909.35	7.5E-04	7.4E-04	1906.62	2.0E-03	2.0E-03 2.0E-03	1901.74	7.6E-04	7.3E-04 7.5E-04				
18.5	1903.98	2.0E-03	1.8E-03 2.0E-03	1908.92	7.2E-04	7.2E-04	1906.04	2.0E-03	2.3E-03 2.0E-03	1901.11	7.3E-04	8.5E-04 7.3E-04				
19.5	1903.47	2.0E-03	2.0E-03	1908.46	6.9E-04	6.9E-04	1905.44	2.0E-03	2.0E-03	1900.46	7.0E-04	7.0E-04	7.0E-04			
20.5	1902.93	2.0E-03	2.1E-03	1907.99	6.7E-04	6.7E-04	1904.83	2.0E-03	2.0E-03	1899.79	6.8E-04	6.8E-04				

**Notes.**<sup>a</sup> This work.<sup>b</sup> First entry: deduced from integrated cross sections of Yoshino et al. (2006). Second entry: deduced from Einstein emission coefficients of Qu et al. (2021a).

**Table 3**  
Transition Energies (in Å) and Line Oscillator Strengths for  $Q_{11}$ ,  $Q_{12}$ ,  $Q_{22}$ , and  $Q_{21}$  branches of the  $C^2\Pi(0)$ - $X^2\Pi(0)$  band of NO

$J''$	$Q_{11}$			$Q_{12}$			$Q_{22}$			$Q_{21}$		
	$\lambda^a$	$f^a$	$f^b$									
1.5	1909.31	1.8E-04	2.1E-04	1913.69	1.7E-03	9.0E-04	1913.24	2.6E-04	8.2E-05	1908.86	3.2E-05	1.9E-06
2.5	1909.21	7.3E-05	7.0E-05	1913.60	5.8E-04	3.7E-04	1913.32	2.5E-04	1.5E-04	1908.93	2.5E-05	7.3E-06
3.5	1909.22	2.1E-05	2.3E-05	1913.62	1.5E-04	4.6E-05	1913.32	3.2E-04	2.6E-04	1908.92	2.7E-05	1.8E-05
4.5	1909.34	1.7E-05	1.8E-05	1913.76	1.1E-04	6.2E-06	1913.19	2.4E-04	2.2E-04	1908.78	1.7E-05	1.5E-05
5.5	1909.40	2.5E-05	2.4E-05	1913.84	1.4E-04	8.6E-05	1913.03	1.7E-04	1.6E-04	1908.59	1.1E-05	9.8E-06
6.5	1909.36	2.2E-05	2.1E-05	1913.82	1.1E-04	9.4E-05	1912.83	1.3E-04	1.2E-04	1908.38	7.1E-06	6.6E-06
7.5	1909.28	1.8E-05	1.7E-05	1913.76	8.8E-05	7.8E-05	1912.62	9.7E-05	9.5E-05	1908.14	4.8E-06	4.5E-06
8.5	1909.16	1.5E-05	1.5E-05	1913.67	6.8E-05	6.3E-05	1912.38	7.7E-05	7.6E-05	1907.87	3.3E-06	3.1E-06
9.5	1909.02	1.3E-05	1.3E-05	1913.56	5.4E-05	5.2E-05	1912.12	6.3E-05	6.2E-05	1907.59	2.3E-06	2.2E-06
10.5	1908.85	1.1E-05	1.1E-05	1913.43	4.4E-05	4.2E-05	1911.85	5.2E-05	5.2E-05	1907.27	1.7E-06	1.6E-06
11.5	1908.67	1.0E-05	9.8E-06	1913.28	3.7E-05	3.5E-05	1911.55	4.4E-05	4.4E-05	1906.94	1.2E-06	1.1E-06
12.5	1908.45	8.9E-06	8.8E-06	1913.11	3.1E-05	3.0E-05	1911.24	3.8E-05	3.8E-05	1906.59	8.7E-07	8.3E-07
13.5	1908.22	8.0E-06	8.0E-06	1912.92	2.6E-05	2.5E-05	1910.90	3.3E-05	3.3E-05	1906.21	6.3E-07	6.0E-07
14.5	1907.96	7.3E-06	7.3E-06	1912.71	2.2E-05	2.2E-05	1910.54	2.9E-05	2.9E-05	1905.81	4.5E-07	4.3E-07
15.5	1907.68	6.7E-06	6.7E-06	1912.48	1.9E-05	1.9E-05	1910.17	2.5E-05	2.5E-05	1905.38	3.3E-07	3.1E-07
16.5	1907.38	6.2E-06	6.1E-06	1912.23	1.7E-05	1.7E-05	1909.77	2.2E-05	2.2E-05	1904.94	2.3E-07	2.2E-07
17.5	1907.06	5.7E-06	5.7E-06	1911.96	1.5E-05	1.5E-05	1909.36	2.0E-05	2.0E-05	1904.47	1.6E-07	1.5E-07
18.5	1906.71	5.3E-06	5.3E-06	1911.67	1.3E-05	1.3E-05	1908.92	1.8E-05	1.8E-05	1903.98	1.1E-07	1.0E-07
19.5	1906.34	5.0E-06	4.9E-06	1911.36	1.2E-05	1.2E-05	1908.47	1.6E-05	1.6E-05	1903.47	7.4E-08	6.9E-08
20.5	1905.95	4.6E-06	4.6E-06	1911.02	1.0E-05	1.0E-05	1908.00	1.5E-05	1.5E-05	1902.94	4.7E-08	4.4E-08

**Notes.**<sup>a</sup> This work.<sup>b</sup> Deduced from Einstein emission coefficients of Qu et al. (2021a).

previous ones. Therefore, we have taken the molecular constants given by Amiot & Verges (1982) for the  $C^2\Pi(0)$  Rydberg state and those of Murray et al. (1994) for the  $B^2\Pi(7)$  valence state.

The coupling parameters of the  $B^2\Pi(7)$  and  $C^2\Pi(0)$  states are presently obtained by fitting the eigenvalues to the term values derived from high-resolution Fourier transform spectroscopic measurements for  $e$  and  $f$   $\Lambda$ -doubling components of the rotational levels of the four states involved in the interaction. Term values have been reported for the  $C^2\Pi_{1/2}(0)$  and  $C^2\Pi_{3/2}(0)$  states up to  $J = 26.5$  (Braun et al. 2000), and for the  $B^2\Pi_{1/2}(7)$  and  $B^2\Pi_{3/2}(7)$  states up to  $J$  values of 8.5 and 7.5, respectively (Murray et al. 1994). Using a value of  $3.5 \text{ cm}^{-1}$  for the coupling parameters between the two doublet components of the  $C^2\Pi$  state and the two doublet components of the  $B^2\Pi$  state, the mean absolute deviation between the computed and empirical set of term values is  $0.08 \text{ cm}^{-1}$ .

When rotational perturbations are present, Equation (2) is no longer appropriate. If the upper state of the transition is perturbed by  $J'$ -dependent interactions with other states, an adequate model of the rovibronic structure in the absorption spectra requires to consider the interaction between the rotational excited states. According to Walter et al. (2000), each perturbed electronic state of a rovibrational level may be represented by an appropriate linear combination of diabatic unperturbed basis states, and the line strength of a rovibronic transition can be written as follows:

$$S_{J'J''} = \left| \sum_k C_k \langle v'_k | v'' \rangle R_e^k (\mathcal{J}_{J'J''})^{1/2} \right|^2 \quad (7)$$

where  $R_e^k$  is the electronic moment between the lower electronic state and the upper  $k_{th}$  diabatic state and  $\langle v'_k | v'' \rangle$  is

the vibrational overlap integral.  $C_k$  is the coefficient of the  $k_{th}$  basis state.

As already mentioned, the Rydberg  $C^2\Pi(0)$  state is perturbed by the valence  $B^2\Pi(7)$  state. The fractional weights of  $C^2\Pi$  character in the perturbed rovibronic state  $i$  ( $C^2\Pi_{1/2}$ ,  $C^2\Pi_{3/2}$ ) (Ackerman & Miescher 1969) may be written as:

$$C^2 = s_{iC1}^2 + s_{iC2}^2, \quad (8)$$

where  $s_{iC1}$  and  $s_{iC2}$  are, respectively, the eigenvectors for the  $C^2\Pi_{1/2}(0)$  and  $C^2\Pi_{3/2}(0)$  basis states in the state  $i$ . Analogously, the fractional weights of  $B^2\Pi$  character in the perturbed rovibronic state  $i$  can be expressed as:

$$B^2 = s_{iB1}^2 + s_{iB2}^2, \quad (9)$$

where  $s_{iB1}$  and  $s_{iB2}$  are, respectively, the eigenvectors for the  $B^2\Pi_{1/2}(7)$  and  $B^2\Pi_{3/2}(7)$  basis states in the state  $i$ . The  $s_{iC1}$ ,  $s_{iC2}$ ,  $s_{iB1}$ , and  $s_{iB2}$  eigenvectors are obtained in the previously described diabatic state mixing model. In this way, to take into account the  $C^2\Pi \sim B^2\Pi$  interaction in our calculations, we have adopted the following expression for the line strength:

$$S_{J'J''} = [C \langle v'_C | v'' \rangle R_e^C (\mathcal{J}_{J'J''})^{1/2} + B \langle v'_B | v'' \rangle R_e^B (\mathcal{J}_{J'J''})^{1/2}]^2, \quad (10)$$

where  $v'_C$ ,  $v'_B$ , and  $v''$  are the vibrational wave functions of the  $C^2\Pi(0)$ ,  $B^2\Pi(7)$ , and ground states, respectively.  $R_e^C$  is the electronic transition moment between the ground and  $C^2\Pi$  electronic states and  $R_e^B$  is the electronic transition moment between the ground and  $B^2\Pi$  electronic states.  $C$  and  $B$  are the square root of the fractional weights of  $C^2\Pi$  and  $B^2\Pi$  characters, respectively, in the perturbed  $C^2\Pi_{1/2}$  and  $C^2\Pi_{3/2}$  states.

**Table 4**  
Transition Energies (in Å) and Line Oscillator Strengths for the  $C^2\Pi(0) - X^2\Pi(1)$  band of NO

$J''$	$P_{11}$		$P_{12}$		$R_{11}$		$R_{12}$		$Q_{11}$		$Q_{12}$	
	$\lambda$	$f$										
1.5					1979.81	1.6E-03	1984.51	1.1E-03	1980.24	2.5E-04	1984.94	2.3E-03
2.5	1980.56	1.4E-03	1985.28	9.6E-04	1979.68	5.1E-04	1984.39	4.0E-04	1980.13	9.2E-05	1984.85	7.2E-04
3.5	1980.59	1.2E-03	1985.32	9.2E-04	1979.67	6.4E-04	1984.40	5.0E-04	1980.14	1.8E-05	1984.86	1.3E-04
4.5	1980.72	4.2E-04	1985.46	3.1E-04	1979.61	1.8E-03	1984.34	1.4E-03	1980.26	1.6E-05	1985.00	9.8E-05
5.5	1980.97	5.5E-04	1985.74	4.0E-04	1979.42	2.3E-03	1984.18	1.7E-03	1980.32	3.2E-05	1985.08	1.9E-04
6.5	1981.16	1.6E-03	1985.95	1.1E-03	1979.19	2.5E-03	1983.97	1.7E-03	1980.27	3.2E-05	1985.05	1.7E-04
7.5	1981.24	2.1E-03	1986.06	1.4E-03	1978.93	2.6E-03	1983.73	1.7E-03	1980.16	2.7E-05	1984.98	1.3E-04
8.5	1981.27	2.3E-03	1986.12	1.4E-03	1978.63	2.7E-03	1983.47	1.6E-03	1980.03	2.3E-05	1984.87	1.1E-04
9.5	1981.26	2.4E-03	1986.15	1.4E-03	1978.31	2.7E-03	1983.18	1.6E-03	1979.86	2.0E-05	1984.74	8.5E-05
10.5	1981.23	2.5E-03	1986.15	1.4E-03	1977.96	2.8E-03	1982.87	1.5E-03	1979.67	1.8E-05	1984.59	7.0E-05
11.5	1981.16	2.6E-03	1986.13	1.4E-03	1977.59	2.9E-03	1982.53	1.5E-03	1979.45	1.6E-05	1984.41	5.8E-05
12.5	1981.08	2.7E-03	1986.08	1.3E-03	1977.19	2.9E-03	1982.18	1.4E-03	1979.21	1.4E-05	1984.21	4.9E-05
13.5	1980.96	2.7E-03	1986.01	1.3E-03	1976.77	3.0E-03	1981.80	1.4E-03	1978.94	1.3E-05	1983.98	4.2E-05
14.5	1980.82	2.8E-03	1985.92	1.2E-03	1976.32	3.0E-03	1981.39	1.3E-03	1978.64	1.2E-05	1983.73	3.6E-05
15.5	1980.65	2.9E-03	1985.81	1.2E-03	1975.84	3.1E-03	1980.97	1.3E-03	1978.32	1.1E-05	1983.46	3.1E-05
16.5	1980.46	2.9E-03	1985.67	1.2E-03	1975.34	3.1E-03	1980.52	1.2E-03	1977.98	9.9E-06	1983.17	2.7E-05
17.5	1980.24	3.0E-03	1985.51	1.1E-03	1974.82	3.1E-03	1980.05	1.2E-03	1977.60	9.1E-06	1982.85	2.4E-05
18.5	1980.00	3.0E-03	1985.32	1.1E-03	1974.27	3.2E-03	1979.56	1.2E-03	1977.21	8.5E-06	1982.51	2.1E-05
19.5	1979.73	3.1E-03	1985.12	1.1E-03	1973.69	3.2E-03	1979.04	1.1E-03	1976.78	8.0E-06	1982.15	1.9E-05
20.5	1979.44	3.1E-03	1984.88	1.0E-03	1973.09	3.3E-03	1978.50	1.1E-03	1976.33	7.5E-06	1981.77	1.7E-05
$J''$	$P_{22}$		$P_{21}$		$R_{22}$		$R_{21}$		$Q_{22}$		$Q_{21}$	
	$\lambda$	$f$										
1.5					1984.21	3.4E-04	1979.51	5.3E-04	1984.46	1.2E-04	1979.76	1.5E-05
2.5	1984.80	6.0E-05	1980.08	9.6E-05	1984.06	1.5E-03	1979.36	1.7E-03	1984.54	2.1E-04	1979.83	2.1E-05
3.5	1985.01	3.2E-04	1980.28	3.6E-04	1983.79	2.1E-03	1979.07	2.0E-03	1984.53	4.1E-04	1979.81	3.5E-05
4.5	1985.14	1.3E-03	1980.39	1.2E-03	1983.47	2.3E-03	1978.73	2.0E-03	1984.40	3.5E-04	1979.66	2.6E-05
5.5	1985.13	1.8E-03	1980.37	1.5E-03	1983.12	2.4E-03	1978.37	1.9E-03	1984.21	2.6E-04	1979.45	1.7E-05
6.5	1985.08	2.1E-03	1980.29	1.6E-03	1982.74	2.5E-03	1977.97	1.9E-03	1983.99	2.0E-04	1979.21	1.1E-05
7.5	1984.99	2.2E-03	1980.18	1.6E-03	1982.34	2.6E-03	1977.54	1.8E-03	1983.75	1.5E-04	1978.94	7.5E-06
8.5	1984.89	2.3E-03	1980.04	1.5E-03	1981.92	2.7E-03	1977.09	1.7E-03	1983.48	1.2E-04	1978.64	5.2E-06
9.5	1984.75	2.4E-03	1979.87	1.5E-03	1981.48	2.7E-03	1976.61	1.7E-03	1983.19	1.0E-04	1978.32	3.7E-06
10.5	1984.60	2.5E-03	1979.68	1.4E-03	1981.01	2.8E-03	1976.11	1.6E-03	1982.88	8.3E-05	1977.97	2.7E-06
11.5	1984.42	2.6E-03	1979.46	1.4E-03	1980.52	2.8E-03	1975.58	1.5E-03	1982.54	7.0E-05	1977.60	1.9E-06
12.5	1984.21	2.7E-03	1979.22	1.4E-03	1980.01	2.9E-03	1975.03	1.5E-03	1982.19	6.0E-05	1977.20	1.4E-06
13.5	1983.99	2.7E-03	1978.95	1.3E-03	1979.47	2.9E-03	1974.45	1.4E-03	1981.81	5.2E-05	1976.77	1.0E-06
14.5	1983.74	2.8E-03	1978.65	1.3E-03	1978.91	3.0E-03	1973.85	1.4E-03	1981.40	4.6E-05	1976.32	7.3E-07
15.5	1983.47	2.8E-03	1978.33	1.2E-03	1978.33	3.0E-03	1973.22	1.3E-03	1980.98	4.0E-05	1975.85	5.2E-07
16.5	1983.18	2.9E-03	1977.98	1.2E-03	1977.73	3.1E-03	1972.57	1.3E-03	1980.53	3.6E-05	1975.35	3.7E-07
17.5	1982.86	3.0E-03	1977.61	1.1E-03	1977.11	3.1E-03	1971.89	1.2E-03	1980.06	3.2E-05	1974.82	2.6E-07
18.5	1982.52	3.0E-03	1977.21	1.1E-03	1976.46	3.2E-03	1971.19	1.2E-03	1979.56	2.9E-05	1974.27	1.8E-07
19.5	1982.16	3.0E-03	1976.79	1.1E-03	1975.80	3.2E-03	1970.46	1.1E-03	1979.05	2.6E-05	1973.70	1.2E-07
20.5	1981.77	3.1E-03	1976.34	1.0E-03	1975.10	3.3E-03	1969.71	1.1E-03	1978.51	2.4E-05	1973.10	7.6E-08

Figure 1 displays the variation of  $C^2\Pi$ -fraction with  $J$  in the  $C^2\Pi_{1/2}$  and  $C^2\Pi_{3/2}$  perturbed states. As can be seen in the figure, the homogeneous interaction  $C^2\Pi(0) \sim B^2\Pi(7)$  affects only the first few rotational levels of the two doublet components of the  $C^2\Pi(0)$  state of NO. The  $C^2\Pi$ -fraction has a minimum value around  $J = 3.5$  in the  $C^2\Pi_{1/2}$  component; this state is almost pure  $C^2\Pi_{1/2}$  state at  $J$  values greater than 5.5. The  $C^2\Pi_{3/2}$  component is characterized by a change in character from the dominant valence  $B^2\Pi$  state at small  $J$  to the dominant Ryberg  $C^2\Pi$  state at large  $J$ . The change takes place around  $J = 3.5$ .

The calculation of the nonperturbed electronic transition moment  $C^2\Pi-X^2\Pi$  with the MQDO method requires the ionization energy of NO and the electronic energy of the

$C^2\Pi$  state as input. We have taken the ionization energy given by Reiser et al. (1988) and the energy of the  $C^2\Pi$  Rydberg state reported by Brunger et al. (2000). The calculated MQDO electronic transition moment is 0.34 a.u. This value is in good agreement with the CAS-MRCI results at the equilibrium position of Cooper (1982), 0.34 a.u., and Zammit et al. (2022), 0.36 a.u., and with the adjusted empirically CAS-MRCI result of 0.30 a.u. of Qu et al. (2021a, 2021b). On the other part, Galluser & Dressler (1982) derived a  $C^2\Pi-X^2\Pi$  electronic transition dipole moment of 0.31 from absolute oscillator strengths for the  $C^2\Pi(0-2)-X^2\Pi(0)$  bands measured by Bethke (1959). For the  $B^2\Pi-X^2\Pi$  valence transition, we have used the electronic transition moment reported by Galluser & Dressler (1982). The vibrational overlap integrals were derived from the

**Table 5**  
Transition Energies (in Å) and Line Oscillator Strengths for the  $C^2\Pi(0)$  -  $X^2\Pi(2)$  band of NO

$J''$	$P_{11}$		$P_{12}$		$R_{11}$		$R_{12}$		$Q_{11}$		$Q_{12}$	
	$\lambda$	$f$										
1.5					2054.99	2.0E-03	2060.05	1.4E-03	2055.46	2.7E-04	2060.52	2.5E-03
2.5	2055.80	1.5E-03	2060.87	1.0E-03	2054.85	1.0E-03	2059.92	7.8E-04	2055.34	1.1E-04	2060.41	9.0E-04
3.5	2055.82	1.5E-03	2060.91	1.1E-03	2054.84	1.2E-03	2059.92	9.0E-04	2055.34	3.5E-05	2060.42	2.5E-04
4.5	2055.96	8.2E-04	2061.06	6.2E-04	2054.76	2.2E-03	2059.85	1.6E-03	2055.46	2.8E-05	2060.56	1.8E-04
5.5	2056.22	9.9E-04	2061.35	7.2E-04	2054.55	2.4E-03	2059.67	1.7E-03	2055.52	3.8E-05	2060.64	2.2E-04
6.5	2056.42	1.9E-03	2061.57	1.3E-03	2054.29	2.5E-03	2059.43	1.7E-03	2055.45	3.3E-05	2060.60	1.7E-04
7.5	2056.49	2.2E-03	2061.67	1.4E-03	2054.00	2.5E-03	2059.16	1.6E-03	2055.33	2.7E-05	2060.50	1.3E-04
8.5	2056.51	2.3E-03	2061.72	1.4E-03	2053.67	2.6E-03	2058.87	1.6E-03	2055.17	2.3E-05	2060.38	1.0E-04
9.5	2056.49	2.4E-03	2061.74	1.4E-03	2053.31	2.6E-03	2058.54	1.5E-03	2054.98	2.0E-05	2060.22	8.2E-05
10.5	2056.43	2.4E-03	2061.72	1.3E-03	2052.92	2.7E-03	2058.19	1.5E-03	2054.76	1.7E-05	2060.04	6.7E-05
11.5	2056.35	2.5E-03	2061.68	1.3E-03	2052.50	2.7E-03	2057.81	1.4E-03	2054.51	1.5E-05	2059.83	5.5E-05
12.5	2056.24	2.5E-03	2061.62	1.3E-03	2052.05	2.8E-03	2057.41	1.4E-03	2054.23	1.3E-05	2059.59	4.6E-05
13.5	2056.09	2.6E-03	2061.52	1.2E-03	2051.58	2.8E-03	2056.98	1.3E-03	2053.92	1.2E-05	2059.33	3.9E-05
14.5	2055.92	2.6E-03	2061.40	1.2E-03	2051.07	2.8E-03	2056.52	1.3E-03	2053.58	1.1E-05	2059.04	3.4E-05
15.5	2055.72	2.7E-03	2061.25	1.1E-03	2050.54	2.9E-03	2056.04	1.2E-03	2053.21	1.0E-05	2058.73	2.9E-05
16.5	2055.49	2.7E-03	2061.08	1.1E-03	2049.97	2.9E-03	2055.53	1.2E-03	2052.81	9.3E-06	2058.39	2.5E-05
17.5	2055.23	2.8E-03	2060.88	1.1E-03	2049.38	3.0E-03	2055.00	1.1E-03	2052.38	8.6E-06	2058.02	2.2E-05
18.5	2054.94	2.8E-03	2060.65	1.0E-03	2048.76	3.0E-03	2054.44	1.1E-03	2051.93	8.0E-06	2057.62	2.0E-05
19.5	2054.62	2.9E-03	2060.40	9.9E-04	2048.11	3.0E-03	2053.86	1.0E-03	2051.44	7.4E-06	2057.21	1.8E-05
20.5	2054.27	2.9E-03	2060.12	9.5E-04	2047.44	3.1E-03	2053.25	1.0E-03	2050.93	7.0E-06	2056.76	1.6E-05
$J''$	$P_{22}$		$P_{21}$		$R_{22}$		$R_{21}$		$Q_{22}$		$Q_{21}$	
	$\lambda$	$f$										
1.5					2059.72	6.7E-04	2054.67	1.1E-03	2060.00	4.6E-04	2054.94	5.5E-05
2.5	2060.35	2.2E-04	2055.28	3.6E-04	2059.56	1.7E-03	2054.50	2.0E-03	2060.08	4.2E-04	2055.01	4.1E-05
3.5	2060.58	6.4E-04	2055.50	7.1E-04	2059.27	2.1E-03	2054.19	2.1E-03	2060.06	5.0E-04	2054.98	4.2E-05
4.5	2060.71	1.5E-03	2055.61	1.4E-03	2058.91	2.3E-03	2053.82	2.0E-03	2059.91	3.6E-04	2054.81	2.7E-05
5.5	2060.69	1.9E-03	2055.57	1.6E-03	2058.53	2.3E-03	2053.41	1.9E-03	2059.70	2.6E-04	2054.58	1.7E-05
6.5	2060.63	2.1E-03	2055.48	1.6E-03	2058.11	2.4E-03	2052.98	1.8E-03	2059.45	1.9E-04	2054.31	1.1E-05
7.5	2060.52	2.2E-03	2055.35	1.5E-03	2057.67	2.5E-03	2052.51	1.7E-03	2059.18	1.5E-04	2054.01	7.2E-06
8.5	2060.39	2.2E-03	2055.19	1.5E-03	2057.20	2.5E-03	2052.01	1.6E-03	2058.88	1.2E-04	2053.68	5.0E-06
9.5	2060.24	2.3E-03	2054.99	1.4E-03	2056.71	2.6E-03	2051.48	1.6E-03	2058.55	9.5E-05	2053.32	3.5E-06
10.5	2060.05	2.4E-03	2054.77	1.4E-03	2056.19	2.6E-03	2050.92	1.5E-03	2058.20	7.9E-05	2052.93	2.5E-06
11.5	2059.84	2.4E-03	2054.52	1.3E-03	2055.64	2.7E-03	2050.34	1.4E-03	2057.82	6.6E-05	2052.51	1.8E-06
12.5	2059.60	2.5E-03	2054.24	1.3E-03	2055.07	2.7E-03	2049.73	1.4E-03	2057.42	5.7E-05	2052.06	1.3E-06
13.5	2059.34	2.6E-03	2053.93	1.2E-03	2054.47	2.8E-03	2049.08	1.3E-03	2056.99	4.9E-05	2051.58	9.4E-07
14.5	2059.05	2.6E-03	2053.58	1.2E-03	2053.85	2.8E-03	2048.41	1.3E-03	2056.53	4.3E-05	2051.08	6.8E-07
15.5	2058.74	2.7E-03	2053.22	1.2E-03	2053.20	2.9E-03	2047.71	1.2E-03	2056.05	3.8E-05	2050.54	4.9E-07
16.5	2058.39	2.7E-03	2052.82	1.1E-03	2052.53	2.9E-03	2046.99	1.2E-03	2055.54	3.4E-05	2049.98	3.5E-07
17.5	2058.03	2.8E-03	2052.39	1.1E-03	2051.83	2.9E-03	2046.23	1.1E-03	2055.01	3.0E-05	2049.39	2.4E-07
18.5	2057.63	2.8E-03	2051.94	1.0E-03	2051.11	3.0E-03	2045.45	1.1E-03	2054.45	2.7E-05	2048.77	1.7E-07
19.5	2057.21	2.9E-03	2051.45	1.0E-03	2050.36	3.0E-03	2044.64	1.1E-03	2053.86	2.5E-05	2048.12	1.1E-07
20.5	2056.77	2.9E-03	2050.94	9.7E-04	2049.58	3.0E-03	2043.80	1.0E-03	2053.25	2.2E-05	2047.45	7.1E-08

RKR curves generated with the spectroscopic constants reported by Engleman & Rouse (1971) and by Galluser & Dressler (1982).

The  $C^2\Pi$ - $X^2\Pi$  bands consist of 12 branches:  $P_{11}$ ,  $Q_{11}$ ,  $R_{11}$ ,  $P_{12}$ ,  $Q_{12}$ ,  $R_{12}$ ,  $P_{22}$ ,  $Q_{22}$ ,  $R_{22}$ ,  $P_{21}$ ,  $R_{21}$ , and  $Q_{21}$ . In the notation used here, the first subscript represents one of the two excited spin-split states and the second subscript represents one of the two ground spin-split states. The Hönl-London factors were calculated from the formulas reported by Kovács (1969) for a doublet-doublet transition with  $\Delta\Lambda = 0$ , in the intermediate coupling case between Hund's case (a) and (b). In order to account for the doublet  $\Lambda$  components, an additional factor of 2 was introduced in each formula.

The absorption oscillator strengths and the transition wavelengths, calculated taking into account the  $C^2\Pi(0)$

$\sim B^2\Pi(7)$  interaction, for the rotational lines of the  $C^2\Pi(0)$ - $X^2\Pi(0-6)$  transitions, are listed in Tables 1–9. We determine the line positions by subtracting the appropriate ground state term from each perturbed rovibronic term presently calculated. Term values for the ground state were taken from Hinz et al. (1986) and Amiot (1982). The terms used in the line positions calculations are mean values for the  $e$  and  $f$   $\Lambda$ -doubling components. The presently calculated line positions agree well with those reported by Qu et al. (2021a), with a mean absolute deviation of  $0.08 \text{ cm}^{-1}$ .

It should be noted that, if the perturbing effect of the  $B^2\Pi(7)$  level is not considered, our calculations predict that the oscillator strengths for lines of the  $P_{11}$ ,  $P_{22}$ ,  $R_{11}$ , and  $R_{22}$  main branches increase as the rotational quantum number increases while those of the  $P_{12}$ ,  $P_{21}$ ,  $R_{12}$ , and  $R_{21}$  satellites branches tend

**Table 6**  
Transition Energies (in Å) and Line Oscillator Strengths for the  $C^2\Pi(0)$ — $X^2\Pi(3)$  band of NO

$J''$	$P_{11}$		$P_{12}$		$R_{11}$		$R_{12}$		$Q_{11}$		$Q_{12}$	
	$\lambda$	$f$										
1.5					2134.83	1.2E-03	2140.28	8.0E-04	2135.33	1.7E-04	2140.78	1.6E-03
2.5	2135.70	9.4E-04	2141.16	6.7E-04	2134.68	4.5E-04	2140.13	3.5E-04	2135.20	6.7E-05	2140.66	5.3E-04
3.5	2135.72	8.7E-04	2141.20	6.7E-04	2134.66	5.5E-04	2140.13	4.3E-04	2135.19	1.6E-05	2140.67	1.1E-04
4.5	2135.86	3.7E-04	2141.35	2.8E-04	2134.56	1.3E-03	2140.05	9.9E-04	2135.32	1.3E-05	2140.82	8.3E-05
5.5	2136.14	4.7E-04	2141.66	3.4E-04	2134.33	1.6E-03	2139.84	1.1E-03	2135.38	2.3E-05	2140.89	1.3E-04
6.5	2136.34	1.2E-03	2141.88	8.0E-04	2134.04	1.7E-03	2139.58	1.1E-03	2135.29	2.2E-05	2140.84	1.1E-04
7.5	2136.40	1.4E-03	2141.98	9.4E-04	2133.71	1.7E-03	2139.28	1.1E-03	2135.15	1.8E-05	2140.72	9.0E-05
8.5	2136.41	1.5E-03	2142.02	9.6E-04	2133.34	1.8E-03	2138.94	1.1E-03	2134.97	1.6E-05	2140.57	7.0E-05
9.5	2136.37	1.6E-03	2142.02	9.4E-04	2132.94	1.8E-03	2138.57	1.1E-03	2134.74	1.3E-05	2140.39	5.6E-05
10.5	2136.30	1.7E-03	2141.99	9.2E-04	2132.50	1.8E-03	2138.18	1.0E-03	2134.49	1.2E-05	2140.17	4.6E-05
11.5	2136.19	1.7E-03	2141.93	9.0E-04	2132.03	1.9E-03	2137.75	9.8E-04	2134.20	1.0E-05	2139.93	3.8E-05
12.5	2136.05	1.8E-03	2141.83	8.7E-04	2131.53	1.9E-03	2137.29	9.5E-04	2133.88	9.3E-06	2139.65	3.2E-05
13.5	2135.87	1.8E-03	2141.71	8.5E-04	2131.00	1.9E-03	2136.81	9.1E-04	2133.52	8.4E-06	2139.35	2.7E-05
14.5	2135.66	1.8E-03	2141.55	8.2E-04	2130.43	2.0E-03	2136.29	8.8E-04	2133.13	7.7E-06	2139.01	2.3E-05
15.5	2135.42	1.9E-03	2141.37	7.9E-04	2129.83	2.0E-03	2135.75	8.5E-04	2132.71	7.0E-06	2138.64	2.0E-05
16.5	2135.14	1.9E-03	2141.15	7.7E-04	2129.19	2.0E-03	2135.17	8.2E-04	2132.25	6.5E-06	2138.25	1.8E-05
17.5	2134.83	1.9E-03	2140.91	7.4E-04	2128.53	2.1E-03	2134.57	7.9E-04	2131.77	6.0E-06	2137.82	1.6E-05
18.5	2134.49	2.0E-03	2140.63	7.2E-04	2127.83	2.1E-03	2133.93	7.6E-04	2131.25	5.6E-06	2137.37	1.4E-05
19.5	2134.12	2.0E-03	2140.33	6.9E-04	2127.10	2.1E-03	2133.27	7.3E-04	2130.69	5.2E-06	2136.88	1.2E-05
20.5	2133.71	2.0E-03	2139.99	6.7E-04	2126.34	2.1E-03	2132.58	7.0E-04	2130.11	4.9E-06	2136.37	1.1E-05
$J''$	$P_{22}$		$P_{21}$		$R_{22}$		$R_{21}$		$Q_{22}$		$Q_{21}$	
	$\lambda$	$f$										
1.5					2139.93	3.0E-04	2134.48	4.7E-04	2140.22	1.5E-04	2134.78	1.8E-05
2.5	2140.60	7.3E-05	2135.14	1.2E-04	2139.75	1.0E-03	2143.30	1.2E-03	2140.31	1.9E-04	2134.85	1.8E-05
3.5	2140.84	2.9E-04	2135.37	3.2E-04	2139.42	1.4E-03	2133.96	1.4E-03	2140.29	3.0E-04	2134.81	2.5E-05
4.5	2140.97	9.3E-04	2135.48	8.7E-04	2139.04	1.5E-03	2133.55	1.3E-03	2140.11	2.4E-04	2134.62	1.7E-05
5.5	2140.95	1.2E-03	2135.43	1.0E-03	2138.61	1.6E-03	2133.10	1.3E-03	2139.87	1.7E-04	2134.36	1.1E-05
6.5	2140.87	1.4E-03	2135.32	1.1E-03	2138.15	1.7E-03	2132.62	1.2E-03	2139.60	1.3E-04	2134.06	7.3E-06
7.5	2140.74	1.5E-03	2135.17	1.0E-03	2137.66	1.7E-03	2132.10	1.2E-03	2139.29	1.0E-04	2133.73	5.0E-06
8.5	2140.59	1.5E-03	2134.98	1.0E-03	2137.14	1.7E-03	2131.55	1.1E-03	2138.95	8.0E-05	2133.36	3.5E-06
9.5	2140.40	1.6E-03	2134.76	9.8E-04	2136.59	1.8E-03	2130.97	1.1E-03	2138.59	6.6E-05	2132.95	2.4E-06
10.5	2140.19	1.7E-03	2134.50	9.5E-04	2136.01	1.8E-03	2130.35	1.0E-03	2138.19	5.5E-05	2132.51	1.7E-06
11.5	2139.94	1.7E-03	2134.21	9.2E-04	2135.41	1.9E-03	2129.70	1.0E-03	2137.76	4.6E-05	2132.04	1.3E-06
12.5	2139.66	1.7E-03	2133.89	8.9E-04	2134.77	1.9E-03	2129.02	9.7E-04	2137.30	4.0E-05	2131.54	9.1E-07
13.5	2139.36	1.8E-03	2133.53	8.7E-04	2134.10	1.9E-03	2128.31	9.3E-04	2136.82	3.4E-05	2131.00	6.6E-07
14.5	2139.02	1.8E-03	2133.14	8.4E-04	2133.41	2.0E-03	2127.56	8.9E-04	2136.30	3.0E-05	2130.44	4.8E-07
15.5	2138.65	1.9E-03	2132.72	8.1E-04	2132.68	2.0E-03	2126.78	8.6E-04	2135.75	2.7E-05	2129.83	3.4E-07
16.5	2138.26	1.9E-03	2132.26	7.8E-04	2131.93	2.0E-03	2125.97	8.3E-04	2135.18	2.4E-05	2129.20	2.4E-07
17.5	2137.83	1.9E-03	2131.77	7.5E-04	2131.15	2.1E-03	2125.13	8.0E-04	2134.58	2.1E-05	2128.54	1.7E-07
18.5	2137.38	2.0E-03	2131.25	7.3E-04	2130.34	2.1E-03	2124.26	7.7E-04	2133.94	1.9E-05	2127.84	1.2E-07
19.5	2136.89	2.0E-03	2130.70	7.0E-04	2129.50	2.1E-03	2123.35	7.4E-04	2133.28	1.7E-05	2127.11	7.8E-08
20.5	2136.38	2.0E-03	2130.12	6.8E-04	2128.63	2.1E-03	2122.41	7.1E-04	2132.59	1.6E-05	2126.35	5.0E-08

to decrease. Furthermore, the intensity of satellite branches is small compared to that of the main branches. On the other hand, the intensity of the four  $Q$  branches decreases rapidly with increasing  $J$ . As can be seen in Tables 1–9 when the perturbation is taken into account, our calculations show important deviations from predictions based in the Hönl–London distribution for the lowest  $J$  values. Oscillator strengths for rovibronic transitions ending in the  $J = 3.5$  and  $4.5$  levels of the  $C^2\Pi_{1/2}$  state, where it is mainly  $B^2\Pi$ , are anomalously weak. Such a decrease of the  $f$ -values can be explained in terms of the perturbation exercised by the  $B^2\Pi_{3/2}(7)$  state since the vibronic transition moment for the  $B^2\Pi(7)$ – $X^2\Pi(0)$  band is much smaller than it is for the  $C^2\Pi(0)$ – $X^2\Pi(0)$  band. Regarding to transitions ending in the two lowest  $J$  levels of the  $C^2\Pi_{3/2}$  state, the low  $f$ -values of the  $P$  and  $R$  branches can be attributed

to the predominantly  $B^2\Pi(7)$  valence character of such levels. Lines with  $J > 5.5$  of the  $C^2\Pi(0)$  state, for which the perturbation is negligible, show a normal Hönl–London distribution intensity pattern.

As far as we know, there are no other theoretical or experimental line  $f$ -values against which we can compare our results. Nonetheless, the integrated cross sections of individual rotational lines measured at 295 K by Yoshino et al. (2006) for the  $C^2\Pi(0)$ – $X^2\Pi(0)$  transition, can be converted into line oscillator strengths through the following expression (Nicholls 1969):

$$f_{J'J''} = \frac{mc^2}{\pi e^2} \frac{1}{N_{J''}/N_{\text{tot}}} \int_{J'J''} \sigma(\nu) d\nu, \quad (11)$$

where the frequency,  $\nu$ , is expressed in wavenumber and  $N_{J''}/N_{\text{tot}}$  is the relative population of the rotational-level  $J''$  of the

**Table 7**  
Transition Energies (in Å) and Line Oscillator Strengths for the  $C^2\Pi(0)$ — $X^2\Pi(4)$  band of NO

$J''$	$P_{11}$		$P_{12}$		$R_{11}$		$R_{12}$		$Q_{11}$		$Q_{12}$	
	$\lambda$	$f$										
1.5					2219.75	6.1E-04	2225.63	4.2E-04	2220.29	9.6E-05	2226.17	9.0E-04
2.5	2220.68	5.3E-04	2226.58	3.7E-04	2219.57	2.0E-04	2225.46	1.6E-04	2220.14	3.6E-05	2226.03	2.8E-04
3.5	2220.70	4.6E-04	2226.61	3.5E-04	2219.55	2.5E-04	2225.45	2.0E-04	2220.13	7.0E-06	2226.03	4.9E-05
4.5	2220.84	1.6E-04	2226.77	1.2E-04	2219.44	7.1E-04	2225.36	5.3E-04	2220.26	6.1E-06	2226.19	3.8E-05
5.5	2221.13	2.2E-04	2227.08	1.6E-04	2219.18	9.0E-04	2225.13	6.5E-04	2220.31	1.3E-05	2226.26	7.2E-05
6.5	2221.33	6.3E-04	2227.32	4.3E-04	2218.85	9.7E-04	2224.83	6.6E-04	2220.21	1.2E-05	2226.19	6.5E-05
7.5	2221.39	8.2E-04	2227.41	5.3E-04	2218.48	1.0E-03	2224.49	6.5E-04	2220.04	1.1E-05	2226.05	5.2E-05
8.5	2221.38	8.9E-04	2227.44	5.5E-04	2218.07	1.0E-03	2224.11	6.3E-04	2219.83	9.1E-06	2225.87	4.1E-05
9.5	2221.33	9.4E-04	2227.42	5.5E-04	2217.62	1.1E-03	2223.69	6.2E-04	2219.57	7.8E-06	2225.66	3.3E-05
10.5	2221.23	9.7E-04	2227.37	5.4E-04	2217.13	1.1E-03	2223.25	6.0E-04	2219.28	6.9E-06	2225.40	2.7E-05
11.5	2221.09	1.0E-03	2227.28	5.3E-04	2216.60	1.1E-03	2222.76	5.7E-04	2218.95	6.1E-06	2225.12	2.2E-05
12.5	2220.92	1.0E-03	2227.16	5.1E-04	2216.04	1.1E-03	2222.25	5.5E-04	2218.57	5.5E-06	2224.80	1.9E-05
13.5	2220.71	1.1E-03	2227.00	5.0E-04	2215.44	1.1E-03	2221.70	5.4E-04	2218.17	4.9E-06	2224.44	1.6E-05
14.5	2220.46	1.1E-03	2226.81	4.8E-04	2214.80	1.2E-03	2221.12	5.2E-04	2217.72	4.5E-06	2224.06	1.4E-05
15.5	2220.17	1.1E-03	2226.58	4.7E-04	2214.12	1.2E-03	2220.50	5.0E-04	2217.24	4.1E-06	2223.63	1.2E-05
16.5	2219.84	1.1E-03	2226.32	4.5E-04	2213.41	1.2E-03	2219.85	4.8E-04	2216.72	3.8E-06	2223.18	1.0E-05
17.5	2219.48	1.1E-03	2226.02	4.4E-04	2212.66	1.2E-03	2219.16	4.6E-04	2216.16	3.5E-06	2222.68	9.2E-06
18.5	2219.08	1.2E-03	2225.69	4.2E-04	2211.88	1.2E-03	2218.45	4.4E-04	2215.57	3.3E-06	2222.16	8.1E-06
19.5	2218.64	1.2E-03	2225.32	4.1E-04	2211.06	1.2E-03	2217.70	4.3E-04	2214.94	3.1E-06	2221.60	7.2E-06
20.5	2218.16	1.2E-03	2224.92	3.9E-04	2210.20	1.3E-03	2216.91	4.2E-04	2214.27	2.9E-06	2221.01	6.5E-06
$J''$	$P_{22}$		$P_{21}$		$R_{22}$		$R_{21}$		$Q_{22}$		$Q_{21}$	
	$\lambda$	$f$										
1.5					2225.24	1.3E-04	2219.37	2.1E-04	2225.56	4.9E-05	2219.69	5.9E-06
2.5	2225.97	2.4E-05	2220.08	3.8E-05	2225.05	5.6E-04	2219.16	6.4E-04	2225.65	8.3E-05	2219.76	8.1E-06
3.5	2226.22	1.3E-04	2220.31	1.4E-04	2224.69	7.9E-04	2218.79	7.7E-04	2225.62	1.6E-04	2219.72	1.4E-05
4.5	2226.36	5.0E-04	2220.43	4.7E-04	2224.26	8.8E-04	2218.34	7.7E-04	2225.42	1.3E-04	2219.50	9.9E-06
5.5	2226.32	7.1E-04	2220.37	5.9E-04	2223.79	9.3E-04	2217.85	7.4E-04	2225.16	9.9E-05	2219.21	6.4E-06
6.5	2226.22	8.0E-04	2220.24	6.1E-04	2223.28	9.7E-04	2217.32	7.1E-04	2224.85	7.5E-05	2218.88	4.3E-06
7.5	2226.07	8.5E-04	2220.06	6.0E-04	2222.74	1.0E-03	2216.75	6.9E-04	2224.50	5.9E-05	2218.50	2.9E-06
8.5	2225.89	9.0E-04	2219.84	5.9E-04	2222.16	1.0E-03	2216.14	6.6E-04	2224.12	4.7E-05	2218.09	2.0E-06
9.5	2225.67	9.3E-04	2219.59	5.7E-04	2221.55	1.0E-03	2215.49	6.4E-04	2223.71	3.8E-05	2217.63	1.4E-06
10.5	2225.42	9.7E-04	2219.29	5.6E-04	2220.91	1.1E-03	2214.80	6.1E-04	2223.26	3.2E-05	2217.14	1.0E-06
11.5	2225.13	1.0E-03	2218.96	5.4E-04	2220.23	1.1E-03	2214.08	5.9E-04	2222.78	2.7E-05	2216.61	7.4E-07
12.5	2224.81	1.0E-03	2218.59	5.2E-04	2219.52	1.1E-03	2213.32	5.7E-04	2222.26	2.3E-05	2216.05	5.3E-07
13.5	2224.45	1.0E-03	2218.18	5.1E-04	2218.78	1.1E-03	2212.53	5.5E-04	2221.71	2.0E-05	2215.45	3.9E-07
14.5	2224.06	1.1E-03	2217.73	4.9E-04	2218.00	1.2E-03	2211.70	5.3E-04	2221.13	1.8E-05	2214.81	2.8E-07
15.5	2223.64	1.1E-03	2217.25	4.7E-04	2217.19	1.2E-03	2210.83	5.1E-04	2220.51	1.6E-05	2214.13	2.0E-07
16.5	2223.18	1.1E-03	2216.73	4.6E-04	2216.35	1.2E-03	2209.93	4.9E-04	2219.86	1.4E-05	2213.42	1.4E-07
17.5	2222.69	1.1E-03	2216.17	4.4E-04	2215.47	1.2E-03	2208.99	4.7E-04	2219.17	1.2E-05	2212.67	1.0E-07
18.5	2222.17	1.2E-03	2215.58	4.3E-04	2214.56	1.2E-03	2208.01	4.5E-04	2218.45	1.1E-05	2211.88	6.9E-08
19.5	2221.61	1.2E-03	2214.95	4.1E-04	2213.62	1.2E-03	2207.00	4.3E-04	2217.70	1.0E-05	2211.06	4.6E-08
20.5	2221.02	1.2E-03	2214.28	4.0E-04	2212.64	1.3E-03	2205.96	4.2E-04	2216.92	9.2E-06	2210.21	2.9E-08

lower state. We assumed a Boltzmann distribution for the rotational-level populations. The oscillator strengths so calculated are also included in Tables 1–3.

Our theoretical predictions for the line oscillator strengths of the  $C^2\Pi(0)$ - $X^2\Pi(0)$  band are in good agreement with those derived from high-resolution measurements of Yoshino et al. (2006) for most of the rotational lines. However, significant discrepancies exist for some low  $J$  values of  $P$  and  $R$  branches. Their  $f$ -values for the  $P_{11}(5.5)$ ,  $R_{11}(2.5)$ , and  $R_{11}(3.5)$  are around twice the present values. For such lines, it seems that the values obtained from experimental data do not reflect the strong interaction Rydberg-valence around  $J = 3.5$  of the  $C^2\Pi_{1/2}$  component of the  $C^2\Pi$  state; indeed, they are closest to our “unperturbed” results. We would remark that the minimum

in the  $C^2\Pi$ -fraction of the  $C^2\Pi_{1/2}$  state has also been found in previous studies on the perturbation of the  $C^2\Pi(0)$  state by the  $B^2\Pi(7)$  state (Ackerman & Miescher 1969). Our  $f$ -values for the  $P_{22}(2.5)$  and  $P_{22}(3.5)$  lines are lower than the comparative ones, which seem to be too large if it is taken into account the predominantly valence  $B^2\Pi(7)$  character of the  $J = 1.5$  and  $2.5$  levels of the  $C^2\Pi_{3/2}$  component. It should be mentioned that the  $P_{22}(2.5)$  and  $P_{22}(3.5)$  lines observed in the spectrum obtained by Yoshino et al. (2006) appear as blended; this feature may explain the discrepancies between our results and those obtained from experimental measurements. On the other hand, our values disagree with the experimental derived  $f$ -values for the rotational lines of the  $P_{21}$  branch with  $J > 13.5$ . It is worth noting that the experimental results deviate from

**Table 8**  
Transition Energies (in Å) and Line Oscillator Strengths for the  $C^2\Pi(0)-X^2\Pi(5)$  band of NO

$J''$	$P_{11}$		$P_{12}$		$R_{11}$		$R_{12}$		$Q_{11}$		$Q_{12}$	
	$\lambda$	$f$										
1.5					2310.20	4.7E-04	2316.56	3.2E-04	2310.79	6.1E-05	2317.15	5.8E-04
2.5	2311.21	3.4E-04	2317.58	2.4E-04	2310.01	2.6E-04	2316.38	2.1E-04	2310.63	2.7E-05	2317.00	2.1E-04
3.5	2311.22	3.5E-04	2317.61	2.7E-04	2309.98	3.0E-04	2316.36	2.3E-04	2310.60	9.3E-06	2316.99	6.5E-05
4.5	2311.37	2.2E-04	2317.78	1.6E-04	2309.85	5.0E-04	2316.25	3.8E-04	2310.74	7.2E-06	2317.14	4.5E-05
5.5	2311.67	2.6E-04	2318.11	1.8E-04	2309.56	5.5E-04	2315.98	3.9E-04	2310.78	8.9E-06	2317.21	5.1E-05
6.5	2311.88	4.5E-04	2318.35	3.1E-04	2309.20	5.5E-04	2315.65	3.8E-04	2310.66	7.5E-06	2317.12	3.9E-05
7.5	2311.93	4.9E-04	2318.43	3.2E-04	2308.78	5.6E-04	2315.26	3.6E-04	2310.46	6.0E-06	2316.96	2.9E-05
8.5	2311.90	5.1E-04	2318.45	3.1E-04	2308.32	5.6E-04	2314.84	3.5E-04	2310.22	5.0E-06	2316.75	2.3E-05
9.5	2311.83	5.2E-04	2318.41	3.0E-04	2307.81	5.7E-04	2314.37	3.3E-04	2309.92	4.3E-06	2316.50	1.8E-05
10.5	2311.70	5.3E-04	2318.33	2.9E-04	2307.26	5.8E-04	2313.87	3.2E-04	2309.59	3.7E-06	2316.21	1.5E-05
11.5	2311.53	5.4E-04	2318.21	2.8E-04	2306.67	5.9E-04	2313.32	3.1E-04	2309.21	3.3E-06	2315.87	1.2E-05
12.5	2311.32	5.5E-04	2318.06	2.7E-04	2306.04	6.0E-04	2312.74	3.0E-04	2308.78	2.9E-06	2315.50	1.0E-05
13.5	2311.07	5.6E-04	2317.86	2.7E-04	2305.36	6.1E-04	2312.12	2.8E-04	2308.31	2.6E-06	2315.09	8.5E-06
14.5	2310.77	5.7E-04	2317.62	2.6E-04	2304.64	6.1E-04	2311.46	2.7E-04	2307.81	2.4E-06	2314.64	7.3E-06
15.5	2310.43	5.8E-04	2317.34	2.5E-04	2303.88	6.2E-04	2310.76	2.6E-04	2307.25	2.2E-06	2314.15	6.3E-06
16.5	2310.04	5.9E-04	2317.03	2.4E-04	2303.08	6.3E-04	2310.02	2.5E-04	2306.66	2.0E-06	2313.63	5.5E-06
17.5	2309.62	6.0E-04	2316.67	2.3E-04	2302.24	6.4E-04	2309.25	2.4E-04	2306.03	1.9E-06	2313.06	4.8E-06
18.5	2309.15	6.1E-04	2316.28	2.2E-04	2301.35	6.5E-04	2308.44	2.3E-04	2305.35	1.7E-06	2312.46	4.3E-06
19.5	2308.64	6.2E-04	2315.85	2.1E-04	2300.43	6.6E-04	2307.59	2.3E-04	2304.63	1.6E-06	2311.81	3.8E-06
20.5	2308.09	6.3E-04	2315.37	2.1E-04	2299.46	6.6E-04	2306.70	2.2E-04	2303.87	1.5E-06	2311.13	3.4E-06
$J''$	$P_{22}$		$P_{21}$		$R_{22}$		$R_{21}$		$Q_{22}$		$Q_{21}$	
	$\lambda$	$f$										
1.5					2316.14	1.8E-04	2309.79	2.9E-04	2316.49	1.4E-04	2310.14	1.7E-05
2.5	2316.93	6.8E-05	2310.56	1.1E-04	2315.93	4.1E-04	2309.57	4.7E-04	2316.58	1.1E-04	2310.21	1.1E-05
3.5	2317.19	1.7E-04	2310.81	1.9E-04	2315.53	4.8E-04	2309.16	4.6E-04	2316.54	1.2E-04	2310.16	9.9E-06
4.5	2317.33	3.7E-04	2310.92	3.4E-04	2315.06	5.0E-04	2308.66	4.4E-04	2316.32	8.1E-05	2309.92	6.0E-06
5.5	2317.28	4.3E-04	2310.85	3.6E-04	2314.54	5.1E-04	2308.12	4.1E-04	2316.02	5.7E-05	2309.59	3.7E-06
6.5	2317.16	4.5E-04	2310.70	3.5E-04	2313.97	5.3E-04	2307.53	3.9E-04	2315.67	4.2E-05	2309.22	2.4E-06
7.5	2316.98	4.7E-04	2310.49	3.3E-04	2313.37	5.4E-04	2306.90	3.7E-04	2315.28	3.2E-05	2308.80	1.6E-06
8.5	2316.77	4.9E-04	2310.24	3.2E-04	2312.73	5.5E-04	2306.22	3.6E-04	2314.85	2.5E-05	2308.33	1.1E-06
9.5	2316.51	5.0E-04	2309.94	3.1E-04	2312.05	5.6E-04	2305.50	3.4E-04	2314.39	2.1E-05	2307.83	7.7E-07
10.5	2316.22	5.2E-04	2309.60	3.0E-04	2311.33	5.7E-04	2304.74	3.3E-04	2313.88	1.7E-05	2307.28	5.5E-07
11.5	2315.89	5.3E-04	2309.22	2.9E-04	2310.58	5.8E-04	2303.94	3.1E-04	2313.33	1.4E-05	2306.68	3.9E-07
12.5	2315.51	5.4E-04	2308.79	2.8E-04	2309.78	5.9E-04	2303.10	3.0E-04	2312.75	1.2E-05	2306.05	2.8E-07
13.5	2315.10	5.6E-04	2308.33	2.7E-04	2308.95	6.0E-04	2302.21	2.9E-04	2312.13	1.1E-05	2305.37	2.0E-07
14.5	2314.65	5.7E-04	2307.82	2.6E-04	2308.08	6.1E-04	2301.28	2.8E-04	2311.47	9.3E-06	2304.65	1.5E-07
15.5	2314.16	5.8E-04	2307.26	2.5E-04	2307.18	6.2E-04	2300.32	2.7E-04	2310.77	8.2E-06	2303.89	1.1E-07
16.5	2313.64	5.9E-04	2306.67	2.4E-04	2306.23	6.3E-04	2299.31	2.6E-04	2310.03	7.3E-06	2303.09	7.5E-08
17.5	2313.07	6.0E-04	2306.03	2.3E-04	2305.25	6.4E-04	2298.26	2.5E-04	2309.26	6.5E-06	2302.25	5.3E-08
18.5	2312.47	6.1E-04	2305.36	2.2E-04	2304.23	6.4E-04	2297.17	2.4E-04	2308.45	5.9E-06	2301.36	3.6E-08
19.5	2311.82	6.2E-04	2304.64	2.2E-04	2303.17	6.5E-04	2296.04	2.3E-04	2307.59	5.3E-06	2300.44	2.4E-08
20.5	2311.14	6.3E-04	2303.88	2.1E-04	2302.08	6.6E-04	2294.87	2.2E-04	2306.70	4.8E-06	2299.47	1.5E-08

predictions based on the Hönl–London distribution for the  $P_{21}$  branch. We have no explanations for this since the rotational levels of the  $C^2\Pi(0)$  at such  $J$  values are not perturbed by the  $B^2\Pi(7)$  state.

On the theoretical part, Qu et al. (2021a) have calculated Einstein emission coefficients for the  $C^2\Pi$ - $X^2\Pi$  band system by using a combination of high-level theory (CAS and MRCI) calculations and experimental absorption cross sections of Yoshino et al. (2006). The Einstein emission coefficients,  $A_{v'J',v''J''}$ , can be converted in line oscillator strength through the equation (Larsson 1983):

$$f_{v'J',v''J''} = \frac{mc}{8\pi^2 e^2} \nu_{v'J',v''J''}^{-2} \frac{2J' + 1}{2J'' + 1} A_{v'J',v''J''}. \quad (12)$$

The oscillator strengths calculated in this way are included in Tables 1–3. Overall, there exists a good agreement between our

results and those of Qu et al. (2021a). However, their results for the  $P_{12}(5.5)$ ,  $P_{21}(2.5)$ ,  $R_{12}(3.5)$ ,  $Q_{12}(4.5)$ , and  $Q_{21}(1.5)$  lines are much lower than the present results. For these lines, we have not found experimental data except for the  $P_{12}(5.5)$  line, for which our result is closer to the experimental value of Yoshino et al. (2006) than that of Qu et al. (2021a). In addition, significant discrepancies are observed between comparative data for some lines at low values of  $J''$ , for instance,  $P_{11}(2.5)$ ,  $P_{22}(2.5)$ , or  $P_{21}(3.5)$ , even though the calculations are scaled to match with the experimental data. It is worth noting that in such cases our results are also closer to the experimental ones. On the other hand, regarding the lines for which there exist discrepancies between the present and experimental results, a reasonably good agreement between our results and those of the ExoMol database is observed.

**Table 9**  
Transition Energies (in Å) and Line Oscillator Strengths for the  $C^2\Pi(0)$ — $X^2\Pi(6)$  band of NO

$J''$	$P_{11}$		$P_{12}$		$R_{11}$		$R_{12}$		$Q_{11}$		$Q_{12}$	
	$\lambda$	$f$										
1.5					2406.73	1.6E-04	2413.61	1.1E-04	2407.36	2.4E-05	2414.25	2.3E-04
2.5	2407.82	1.4E-04	2414.72	9.6E-05	2406.51	6.0E-05	2413.40	4.7E-05	2407.18	8.7E-06	2414.08	7.5E-05
3.5	2407.82	1.2E-04	2414.73	9.5E-05	2406.47	7.3E-05	2413.38	5.7E-05	2407.15	1.7E-06	2414.06	1.5E-05
4.5	2407.97	4.9E-05	2414.91	3.7E-05	2406.32	1.9E-04	2413.25	1.4E-04	2407.29	1.4E-06	2414.22	1.1E-05
5.5	2408.29	6.3E-05	2415.26	4.5E-05	2406.00	2.3E-04	2412.95	1.7E-04	2407.32	3.1E-06	2414.28	1.9E-05
6.5	2408.50	1.6E-04	2415.50	1.1E-04	2405.59	2.4E-04	2412.57	1.7E-04	2407.18	3.1E-06	2414.17	1.7E-05
7.5	2408.54	2.1E-04	2415.58	1.4E-04	2405.12	2.5E-04	2412.14	1.6E-04	2406.95	2.6E-06	2413.98	1.3E-05
8.5	2408.50	2.2E-04	2415.58	1.4E-04	2404.60	2.6E-04	2411.66	1.6E-04	2406.67	2.2E-06	2413.73	1.0E-05
9.5	2408.39	2.4E-04	2415.52	1.4E-04	2404.04	2.6E-04	2411.13	1.5E-04	2406.33	1.9E-06	2413.44	8.2E-06
10.5	2408.24	2.4E-04	2415.41	1.3E-04	2403.42	2.7E-04	2410.56	1.5E-04	2405.94	1.7E-06	2413.10	6.7E-06
11.5	2408.03	2.5E-04	2415.26	1.3E-04	2402.75	2.7E-04	2409.95	1.4E-04	2405.50	1.5E-06	2412.72	5.6E-06
12.5	2407.77	2.6E-04	2415.06	1.3E-04	2402.04	2.8E-04	2409.29	1.4E-04	2405.02	1.4E-06	2412.29	4.7E-06
13.5	2407.47	2.6E-04	2414.82	1.2E-04	2401.28	2.8E-04	2408.59	1.3E-04	2404.48	1.2E-06	2411.81	4.0E-06
14.5	2407.12	2.7E-04	2414.53	1.2E-04	2400.47	2.9E-04	2407.84	1.3E-04	2403.90	1.1E-06	2411.29	3.4E-06
15.5	2406.71	2.7E-04	2414.20	1.2E-04	2399.61	2.9E-04	2407.05	1.2E-04	2403.27	1.0E-06	2410.73	3.0E-06
16.5	2406.26	2.8E-04	2413.82	1.1E-04	2398.71	3.0E-04	2406.22	1.2E-04	2402.60	9.4E-07	2410.13	2.6E-06
17.5	2405.77	2.8E-04	2413.40	1.1E-04	2397.76	3.0E-04	2405.34	1.1E-04	2401.87	8.7E-07	2409.47	2.3E-06
18.5	2405.22	2.9E-04	2412.93	1.0E-04	2396.77	3.1E-04	2404.42	1.1E-04	2401.10	8.1E-07	2408.78	2.0E-06
19.5	2404.63	2.9E-04	2412.42	1.0E-04	2395.72	3.1E-04	2403.45	1.1E-04	2400.28	7.6E-07	2408.04	1.8E-06
20.5	2403.99	3.0E-04	2411.86	9.7E-05	2394.64	3.1E-04	2402.45	1.0E-04	2399.42	7.1E-07	2407.26	1.6E-06
$J''$	$P_{22}$		$P_{21}$		$R_{22}$		$R_{21}$		$Q_{22}$		$Q_{21}$	
	$\lambda$	$f$										
1.5					2413.16	4.2E-05	2406.28	6.6E-05	2413.53	1.9E-05	2406.65	2.3E-06
2.5	2414.00	9.5E-06	2407.11	1.5E-05	2412.92	1.5E-04	2406.03	1.7E-04	2413.63	2.6E-05	2406.73	2.6E-06
3.5	2414.28	4.0E-05	2407.37	4.4E-05	2412.48	2.0E-04	2405.58	2.0E-04	2413.58	4.3E-05	2406.67	3.6E-06
4.5	2414.42	1.3E-04	2407.49	1.3E-04	2411.96	2.2E-04	2405.04	1.9E-04	2413.33	3.4E-05	2406.40	2.5E-06
5.5	2414.36	1.8E-04	2407.40	1.5E-04	2411.38	2.3E-04	2404.43	1.9E-04	2412.99	2.5E-05	2406.03	1.6E-06
6.5	2414.21	2.0E-04	2407.21	1.5E-04	2410.76	2.4E-04	2403.78	1.8E-04	2412.60	1.9E-05	2405.61	1.1E-06
7.5	2414.01	2.1E-04	2406.98	1.5E-04	2410.09	2.5E-04	2403.08	1.7E-04	2412.16	1.5E-05	2405.14	7.3E-07
8.5	2413.75	2.2E-04	2406.69	1.5E-04	2409.37	2.6E-04	2402.33	1.6E-04	2411.68	1.2E-05	2404.62	5.0E-07
9.5	2413.46	2.3E-04	2406.35	1.4E-04	2408.61	2.6E-04	2401.53	1.6E-04	2411.15	9.6E-06	2404.05	3.6E-07
10.5	2413.12	2.4E-04	2405.96	1.4E-04	2407.81	2.7E-04	2400.68	1.5E-04	2410.58	8.0E-06	2403.43	2.5E-07
11.5	2412.73	2.5E-04	2405.52	1.3E-04	2406.97	2.7E-04	2399.79	1.5E-04	2409.96	6.7E-06	2402.76	1.8E-07
12.5	2412.30	2.5E-04	2405.03	1.3E-04	2406.08	2.8E-04	2398.85	1.4E-04	2409.30	5.8E-06	2402.05	1.3E-07
13.5	2411.82	2.6E-04	2404.50	1.3E-04	2405.15	2.8E-04	2397.86	1.4E-04	2408.60	5.0E-06	2401.29	9.6E-08
14.5	2411.31	2.7E-04	2403.91	1.2E-04	2404.18	2.9E-04	2396.83	1.3E-04	2407.85	4.4E-06	2400.48	7.0E-08
15.5	2410.74	2.7E-04	2403.28	1.2E-04	2403.16	2.9E-04	2395.75	1.3E-04	2407.06	3.9E-06	2399.62	5.0E-08
16.5	2410.14	2.8E-04	2402.61	1.1E-04	2402.10	3.0E-04	2394.62	1.2E-04	2406.23	3.4E-06	2398.72	3.5E-08
17.5	2409.48	2.8E-04	2401.88	1.1E-04	2401.00	3.0E-04	2393.45	1.2E-04	2405.35	3.1E-06	2397.77	2.5E-08
18.5	2408.79	2.9E-04	2401.11	1.1E-04	2399.85	3.0E-04	2392.23	1.1E-04	2404.43	2.8E-06	2396.78	1.7E-08
19.5	2408.05	2.9E-04	2400.29	1.0E-04	2398.67	3.1E-04	2390.97	1.1E-04	2403.46	2.5E-06	2395.73	1.1E-08
20.5	2407.27	3.0E-04	2399.43	9.9E-05	2397.44	3.1E-04	2389.66	1.0E-04	2402.46	2.3E-06	2394.64	7.3E-09

In order to assess the reliability of the present results, we have also calculated the oscillator strength for the  $\delta(0,0)$  band for which previous experimental and theoretical results have been found in the literature. From the calculated line oscillator strengths, we have derived integrated absorption cross sections for the individual rotational lines of the  $C^2\Pi(0)$ - $X^2\Pi(0)$  band through Equation (10). By adding up the integrated absorption cross section contribution for all the rotational lines we have estimated the band oscillator strength through the following equation (Morton & Noreau 1994):

$$f_{v'v''} = \frac{mc^2}{\pi e^2} \int \sigma(v) dv \quad (13)$$

The calculated oscillator strength for the  $\delta(0,0)$  band results to be equal to 0.00238, which conforms very well with the value of 0.00229 obtained by Chan et al. (1993) by using the high-

resolution dipole (e,e) technique and with the value of 0.00234 derived from ultrahigh-resolution photoabsorption measurements by Yoshino et al. (2006). It is worth mentioning that the latest authors estimated an uncertainty of about 5% in their measured band oscillator strength. Regarding the theoretical data available, our result is in reasonable good agreement with the band  $f$ -values of 0.00220 and 0.00249 reported by Galluser & Dressler (1982) and De Vivie & Peyerimhoff (1988), respectively. Zammit et al. (2022) reported a value of 0.0025 for the rotationally averaged absorption oscillator strength of the diabatic  $C^2\Pi(0)$ - $X^2\Pi(0)$  transition. Therefore, the electronic transition moment, overlap integrals, and eigenvector components obtained in this work seem to be accurate.

The absorption oscillator strengths for rotational lines of the  $C^2\Pi(0)$ - $X^2\Pi(1-6)$  bands are displayed in Tables 4–9. The

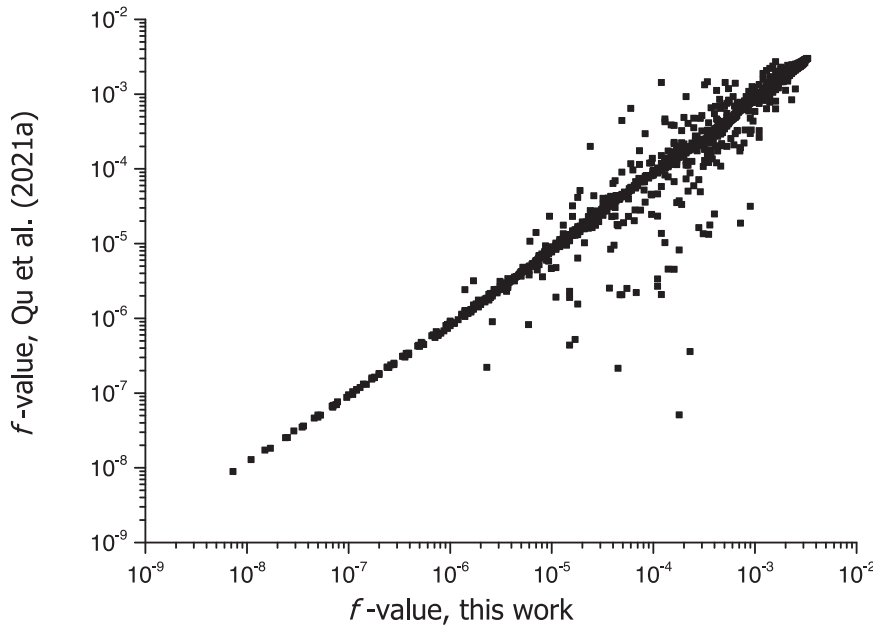


**Figure 2.** A comparative plot of the present  $f$ -values and those deduced from Einstein emission coefficients data of Qu et al. (2021a).

comments we made above in describing the influence of the perturbation on the rotational structure of the  $C^2\Pi(0)-X^2\Pi(0)$  band are applicable to the remaining bands of the  $C^2\Pi(0)-X^2\Pi(v'')$  vibrational progression; this is, a weakening of the intensity of the rotational lines for transitions to the lowest  $J$  values of the  $C^2\Pi(0)$  state as a consequence of the perturbing effect of the  $B^2\Pi(7)$  state. Our calculations predict the  $C^2\Pi(0)-X^2\Pi(1)$  and  $C^2\Pi(0)-X^2\Pi(2)$  to be the most intense bands of de  $C^2\Pi(0)$  progression. The  $f$ -values of the rotational lines of both bands are similar to each other and larger than those of the  $C^2\Pi(0)-X^2\Pi(0)$  band. This fact can be interpreted on the basis of the Franck–Condon principle. According to our calculations, the Franck–Condon overlap is more favorable for the levels  $v'' = 1$  (0.2415) and  $v'' = 2$  (0.2331) of the ground state than for the  $v'' = 0$  level (0.1443). On the other hand, line  $f$ -values of the  $C^2\Pi(0)-X^2\Pi(3)$  band, with a Franck–Condon factor of 0.1701, are similar in magnitude to the corresponding lines of the  $C^2\Pi(0)-X^2\Pi(0)$  band.

No comparative values of experimental character have been found in the literature for the rotational structure of bands with  $v'' > 0$ . As far as we know, the only data of transition intensities at rotational level for such bands are the Einstein emission coefficients reported within the ExoMol database (Qu et al. 2021a). It should be mentioned that these authors scaled their results to experimental measurements of  $\delta(v', v'')$  with  $v'' = 0$ . A comparison of the presently obtained  $f$ -values and those of Qu et al. (2021a) for lines of  $C^2\Pi(0)-X^2\Pi(1-6)$  bands is presented in Figure 2. We observe a reasonable agreement between our calculations and those derived from emission coefficients: on average, about of 20% of the present results for the lines of the  $C^2\Pi(0)-X^2\Pi(2)$  and  $C^2\Pi(0)-X^2\Pi(3)$  bands, and about of 30% for the remaining bands. Qu et al. (2021a) pointed out that their “interaction model for  $B^2\Pi - C^2\Pi$  is not perfect”. For nonperturbed lines, that is, lines with  $J' \geq 5.5$ , the differences between them decrease to about of 10% for the  $\delta(0,1)$  band, 15% for the  $\delta(0,2)$ ,  $\delta(0,3)$ , and  $\delta(0,4)$  bands, and 20% for the  $\delta(0,5)$  and  $\delta(0,6)$  bands.

Summarizing, in this study, we have calculated transition energies and oscillator strengths for rotational lines of the  $C^2\Pi(0)-X^2\Pi(0-6)$  bands in nitric oxide using a model that includes the homogeneous perturbation between the rotational levels of the  $C^2\Pi_{1/2}$ ,  $C^2\Pi_{3/2}$ ,  $B^2\Pi_{1/2}$ , and  $B^2\Pi_{3/2}$  states. As a consequence of the Rydberg–valence interaction, for the lowest  $J$  values, the rotational lines intensities of the seven bands are weaker than the intensities expected from predictions based on Hönl–London factors. According our calculations, the  $C^2\Pi(0)-X^2\Pi(1)$  and  $C^2\Pi(0)-X^2\Pi(2)$  bands are the most intense bands of the  $C^2\Pi(0)-X^2\Pi(v'')$  progression. Our theoretical predictions for the line  $f$ -values of the  $C^2\Pi(0)-X^2\Pi(0)$  band show a general good agreement with those derived from the experimental data reported by Yoshino et al. (2006) and those derived from Einstein emission coefficients reported within the ExoMol database (Qu et al. 2021a). Note that Qu et al. (2021a) scaled their theoretical results in order to match with the measurements of Yoshino et al. (2006), while our results agree with experimental measurements for the  $C^2\Pi(0)-X^2\Pi(0)$  band with no need for additional scaling. This fact makes us confident in the accuracy of our results for transitions that have not yet been measured, as is the case for bands with  $v'' > 0$ . We hope that the data reported in this work may contribute to a better understanding of the processes taking place on Earth, Venus, and Mars atmospheres.

This work has been supported by the Junta de Castilla y León (UCI 139, Grant VA244P20).

## ORCID iDs

C. Lavín <https://orcid.org/0000-0002-8104-2805>  
A. M. Velasco <https://orcid.org/0000-0003-3835-6873>

## References

- Ackerman, F., & Miescher, E. 1969, *JMoSp*, 31, 400  
Amiot, C. 1982, *JMoSp*, 94, 150

- Amiot, C., & Verges, J. 1982, *Phys*, **25**, 302
- Bertaux, J.-L., Leblanc, g., Severine, P., et al. 2005, *Sci*, **307**, 566
- Bethke, G. W. 1959, *JChPh*, **31**, 662
- Braun, V. D., Huber, K. P., Vervloet, M., et al. 2000, *JMoSp*, **203**, 65
- Brunger, M. J., Campbell, L., Cartwright, D. C., et al. 2000, *JPhB*, **33**, 783
- Carroll, P. K., & Hagim, Kh. I. 1988, *Phys*, **37**, 682
- Chan, W. F., Cooper, G., Sodhi, R. N. S., & Brion, C. E. 1993, *CP*, **170**, 81
- Chauveau, S., Perrin, M.-Y., Rivière, P., & Soufiani, A. 2002, *JQSR*, **72**, 503
- Cohen-Sabban, J., & Vuillemin, A. 1973, *Ap&SS*, **24**, 127
- Cooper, D. M. 1982, *JQSR*, **27**, 459
- Dana, V., Mandin, J.-Y., Coudert, L. H., et al. 1994, *JMoSp*, **165**, 525
- De Vivie, R., & Peyerimhoff, S. D. 1988, *JChPh*, **89**, 3028
- Eastes, R. W., Huffman, R. E., & Leblanc, F. J. 1992, *P&SS*, **40**, 481
- Engleman, R., & Rouse, P. E. 1971, *JMoSp*, **37**, 240
- Feldman, P. D., Moos, H. W., Clarke, J. T., & Lane, A. L. 1979, *Natur*, **279**, 221
- Feldman, P. D., & Takacs, P. Z. 1974, *GeoRL*, **1**, 169
- Galluser, R., & Dressler, K. 1982, *JChPh*, **76**, 4311
- Gérard, J.-C., Cox, C., Saglam, A., et al. 2008, *JGRE*, **113**, E00B03
- Gerin, M., Viala, Y., Pauzat, F., & Ellinger, Y. 1992, *A&A*, **266**, 463
- Herzberg, G., Lagerqvist, A., & Miescher, E. 1956, *CaJPh*, **34**, 621
- Hinz, A., Wells, J. S., & Maki, A. G. 1986, *JMoSp*, **119**, 120
- Joshi, P. R., Zins, E.-L., & Krim, L. 2012, *MNRAS*, **419**, 1713
- Kato, H., Kawahara, H., Hoshino, M., et al. 2007, *CPL*, **444**, 34
- Klein, O. 1932, *ZPhy*, **76**, 226
- Kovács, I. 1969, Rotational Structure in the Spectra of Diatomic Molecules (New York: Elsevier)
- Lagerqvist, A., & Miescher, E. 1958, *AcHPh*, **31**, 221
- Larsson, M. 1983, *A&A*, **128**, 291
- Lavín, C., & Velasco, A. M. 2011, *ApJ*, **739**, 16
- Liszt, H. S., & Turner, B. E. 1978, *ApJ*, **224**, L73
- Martín, I., Lavín, C., Velasco, A. M., et al. 1996, *CP*, **202**, 307
- Martín, S., Mauersberger, R., Martín-Pintado, J., García-Burillo, S., & Henkel, C. 2003, *A&A*, **411**, L465
- Mayor, E., Velasco, A. M., & Martín, I. 2005, *JChPh*, **123**, 114305
- McGonagle, D., Ziurys, L. M., Irvine, W. M., & Minh, Y. C. 1990, *ApJ*, **359**, 121
- Morton, D. C., & Noreau, L. 1994, *ApJS*, **95**, 301
- Murray, J. E., Yoshino, K., Esmond, J. R., et al. 1994, *JChPh*, **101**, 62
- Nicholls, R. W. 1969, Electronic Spectra of Diatomic Molecules (New York: Elsevier)
- Qu, Q., Cooper, B., Yurchenko, S. N., & Tennyson, J. 2021b, *JChPh*, **154**, 074112
- Qu, Q., Yurchenko, S. N., Tennyson, J., et al. 2021a, *MNRAS*, **504**, 5768
- Quintana-Lacaci, G., Agúndez, M., Cernicharo, J., et al. 2013, *A&A*, **560**, L2
- Rees, A. L. G. 1947, *PPS*, **59**, 998
- Reiser, G., Habenicht, W., Muller-Dethlefs, K., & Schlag, E. W. 1988, *CPL*, **152**, 119
- Rydberg, R. 1931, *ZPh*, **73**, 376
- Scheingraber, H., & Vidal, C. R. 1985, *JOSAB*, **2**, 343
- Stewart, A. I., & Barth, C. A. 1979, *Sci*, **205**, 59
- Velasco, A. M., & Lavín, C. 2020, *ApJ*, **899**, 57
- Velasco, A. M., Lavín, C., Bustos, E., et al. 2010, *JPCA*, **114**, 8450
- Walter, C. W., Cosby, P. C., & Helm, H. 2000, *JChPh*, **112**, 4621
- Whiting, R. E., & Nicholls, R. W. 1974, *ApJS*, **27**, 1
- Yoshino, K., Thorne, A. P., Murray, J. E., et al. 2006, *JChPh*, **124**, 054323
- Zammit, M. C., Leiding, J. A., Colgan, J., et al. 2022, *JPhB*, **55**, 184002
- Ziurys, L. M., McGonagle, D., Minh, Y., & Irvine, W. M. 1991, *ApJ*, **373**, 535